Technical report
TR-162

Ministerie van Verkeer en Waterstaat
Koninklijk Nederlands
Meteorologisch Instituut

TEBEX observations of clouds and radiation -potential and limitations

P. Stammes, A.J. Feijt, A.C.A.P. van Lammeren and G.J. Prangsma

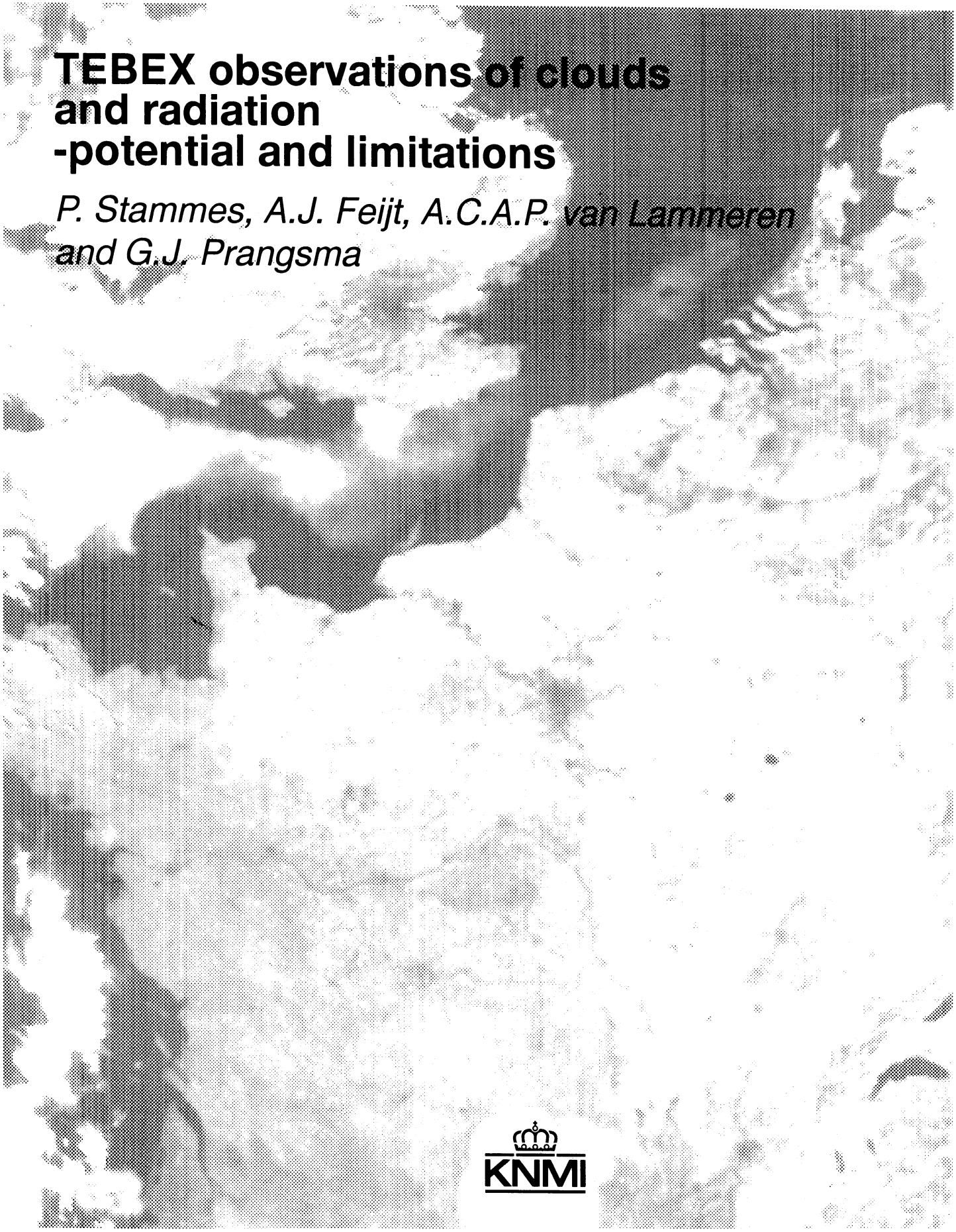

Technical report
TR-162

De Bilt 1994

Postbus 201
3730 AE De Bilt
Wilhelminalaan 10
Telefoon 030-206 911
Telefax 030-210 407

P.Stammes, A.J. Feijt, A.C.A.P. van Lammeren and G.J. Prangsma.

UDC: 551.501.721
551.501.776
551.507.362.2
ISSN: 0169-1708
ISBN: 90-369-2051-5

TEBEX observations of clouds and radiation – potential and limitations

P. Stammes, A.J. Feijt, A.C.A.P. van Lammeren, and G.J. Prangsma

March 1994

Abstract

The Tropospheric Energy and Water Budget Experiment (TEBEX) is an experiment performed by KNMI to observe and model the subgrid variability of atmospheric processes, as relevant for climate models. In the present report we discuss the planned TEBEX observations of clouds and radiation. The aim of the cloud observations is to measure the three-dimensional distribution of clouds and their physical properties over a 130 x 130 km^2 area in the Netherlands. To this purpose a network of cloud detection sites is being installed. These ground observations will be complemented by satellite observations over the same area, using Meteosat and NOAA data. The ground radiation observations will mainly be concentrated at two sites. The satellite observations of radiation are the same as used for the cloud studies. The TEBEX cloud and radiation data will be acquired for a period of two years, starting 1 April 1994.

We also discuss the possibilities and limitations of deriving other, not directly observable cloud and radiation parameters, from the observed quantities. The most important parameters for improving cloud parameterisations in climate models are: the three-dimensional cloud distribution, the distributions of cloud top and cloud base temperature, the distribution of cloud liquid water path, and the relationship between these distribution functions of cloud properties and the radiative fluxes at the surface and the top of the atmosphere. An important aspect of TEBEX is the combination of ground and satellite data to obtain the three-dimensional cloud distribution.

List of contents

1. Introduction

Clouds and radiation are two climatologically important elements of the energy and water budget of the Earth's atmosphere. These and other elements will be observed and modelled in the Tropospheric Energy and Water Budget Experiment, abbreviated as TEBEX, carried out by the Atmospheric Research Section of KNMI. The aims of TEBEX are: (a) to observe energetically relevant physical processes in the atmosphere on a subgrid-scale (i.e., in an area of the order of 100×100 km^2), and (b) to parameterise these processes in terms of grid variables of a regional or global circulation model. The aims of TEBEX are to a large extent similar to those of the GEWEX project (WMO, 1992), which is a part of WCRP (see Appendix A for an explanation of abbreviations).

Since clouds have a large effect on the atmospheric radiation field, and, vice versa, radiation influences the formation of clouds, the two topics are closely linked[1]. Furthermore, the TEBEX cloud detection will be done largely through radiation measurements (viz. remote sensing), so the two topics are also observationally linked. The relationship between clouds and non-radiative transport processes in the troposphere will not be discussed here.

The goal of the TEBEX *cloud observations* is to determine three-dimensional cloud distributions and distribution functions of cloud properties over an area which has approximately the size of a circulation model gridbox. To this purpose a 130×130 km^2 area, with its center at the Cabauw meteorological tower, has been selected. We plan to achieve our goal by a combination of ground and satellite data. Data will be acquired and archived for a period of two years, starting 1 April 1994. The ground observations will be performed by means of a Cloud Detection Network (CDN), consisting of 10 sites in the area under study. The satellite data will come from Meteosat, NOAA-AVHRR and NOAA-TOVS. In this way we can observe clouds with a high spatial and temporal resolution, which is essential because of the natural variability of clouds. It will be interesting to compare in the future the TEBEX cloud and radiation results with ISCCP results for the TEBEX area. The ISCCP project (Schiffer and Rossow, 1983) aims at studying the radiative properties of clouds globally, with a resolution of 250×250 km^2. For the development and testing of subgrid cloud parameterisation in climate models, observations at scales less than about 100 km are needed. As noted by the GEWEX Cloud System Science Team (WMO, 1992, Appendix G), physical processes in cloud systems span all scales, from the synoptic to the microscale. In TEBEX, cloud observations at the microphysical and turbulent scale (less than 1 km), the convective scale (1 to 10 km), and almost the mesoscale (100 km) are performed, but frontal systems and cloud clusters (scale of 1000 km) are not considered. This means that we cannot distinguish organisation in cloud systems on these large scales.

[1]This is also recognized in the Atmospheric Radiation Measurement – ARM – Programme of the U.S.A. (DOE, 1990), which focusses on subgrid variability of radiative energy transport and cloud formation, maintenance and dissipation.

The goal of the TEBEX *radiation observations* is to determine the relationship between SW (shortwave) and LW (longwave) radiative fluxes at the ground and TOA (top-of-the-atmosphere), and cloud parameters, which are found from TEBEX cloud observations. More specifically, the aim is to find the relationship between the radiative fluxes averaged over the TEBEX area and the ensemble properties of clouds over this area. We plan to use global SW radiation measurements at all network sites combined with extensive SW and LW radiation measurements at two sites, Cabauw and Garderen, to find this relationship for the ground fluxes. The satellite data will have to be processed to yield the necessary radiative fluxes at TOA.

The modelling and parameterisation efforts, which form an essential part of TEBEX, will be done in the framework of the development of a Regional Atmospheric Climate Model (RACMO) at KNMI. Especially, the cloud and radiation parameterisations in RACMO can be tested against the TEBEX observations. Furthermore, comparisons can be made between the TEBEX cloud observations and model results from the High Resolution Limited Area Model (HIRLAM[2]), which is a regional weather forecast model operational at KNMI. The interrelations of the various elements of TEBEX regarding clouds and radiation are shown in Fig. 1. These interrelations will be discussed further in this report.

This report describes the status of instrumentation and research plans for TEBEX observations of clouds and radiation on 1 January 1994. The structure of this report is as follows. In Sect. 2 we first give a short list of physical parameters of clouds and radiation, which should ideally be available for cloud and radiation parameterisation in a climate model. In Sect. 3 a brief description of the ground and satellite instruments available for TEBEX will be given. In Sect. 4 the observable cloud parameters will be discussed, as well as derivable parameters which are needed in climate modelling. Also the planned method of analysing the observations will be treated. In Sect. 5 the same will be done for the radiation parameters. The problem of combining ground and satellite data will be briefly discussed in Sect. 6. Discussion and conclusions will be presented in Sect. 7.

[2]The HIRLAM system was developed by the HIRLAM-project group, a cooperative project of Denmark, Finland, Iceland, Ireland, The Netherlands, Norway, and Sweden.

2. Relevant cloud and radiation parameters

In this section we will give an overview of the physical parameters of clouds and radiation that appear to be relevant to adequately represent clouds and radiation in an atmospheric climate model. This list should not be regarded as the realistic aim of the TEBEX observations (see Sects. 4 and 5 for observable parameters), but it is intended as an ideal physical parameter list for clouds and radiation.

2.1 Cloud parameters

The relevant parameters to describe *an individual cloud* are:

(a) *geometric properties* in a Cartesian coordinate system $(\hat{x}, \hat{y}, \hat{z})$, where $\hat{z}$ is the vertical direction:
- size in $\hat{x}$, $\hat{y}$, and $\hat{z}$ directions, denoted by d_x, d_y, and h, respectively
- largest and smallest size in horizontal ($\hat{x}$-$\hat{y}$-) plane, denoted by d_{max} and d_{min}, respectively
- surface area in horizontal plane: A
- cloud base height z_b
- cloud top height z_t.

(b) *macrophysical radiative properties*:
SW range
- (bidirectional) reflectivity $R(\mu, \mu_0, \phi - \phi_0)$; this describes the SW radiance[3] in some spectral band emerging from a cloud in an upward direction (μ, ϕ) for a direction of incidence of the sun (μ_0, ϕ_0), as a fraction of the incident flux[4]; the definitions of the directional coordinates are given in Fig. 2
- (bidirectional) transmissivity $Tr(\mu, \mu_0, \phi - \phi_0)$; this describes the SW radiance in some spectral band emerging from a cloud in a downward direction (μ, ϕ) for a direction of incidence of the sun (μ_0, ϕ_0), as a fraction of the incident flux
- albedo $\rho(\mu_0)$; this is the integral of R, weighted by μ, over all upward directions of emergence
- transmission $\tau(\mu_0)$; this is the integral of Tr, weighted by μ, over all downward directions of emergence
- absorption $\alpha(\mu_0)$; this the difference between unity (i.e. the normalised incident flux) and the sum of $\rho(\mu_0)$ and $\tau(\mu_0)$
- optical thickness τ_0; $\exp(-\tau_0/\mu_0)$ is the fractional extinction of direct sunlight by the cloud

[3]The term radiance is used for: radiative flux density in a specific direction, per unit area perpendicular to this direction, per unit solid angle, in W/(m^2 sr).

[4]The term flux (or irradiance) is used for: radiative flux density on a horizontal surface area, in W/m^2.

LW range

– emissivity ϵ; this is the flux emitted by a cloud divided by the theoretical black-body thermal emission of the cloud, holding for some spectral band. If the emissivity of a cloud is less than one, reflection and/or transmission of incident LW radiation takes place. We can then, analogously to the above, define (bidirectional) LW reflectivity and transmissivity, and LW albedo and transmission.

(c) *other macrophysical properties:*
– liquid water path W (i.e. column density of liquid water)
– ice path I
– cloud base temperature T_b
– cloud top temperature T_t
– water vapour path.

(d) *microphysical properties:*
– particle number density n
– particle size distribution $n(r)$, where r is the particle radius
– effective particle radius r_e
– particle phase (water/ice)
– particle shape (in case of ice particles)
– precipitation rate
– concentration of cloud condensation nuclei (CCN) and aerosols
– concentration of ice nuclei (IN)
– vertical profiles of these microphysical quantities.
Note that the above parameters are not all independent; e.g. the cloud liquid water path can be derived from the vertical profile of particle size and number density.

Actually, it is not very practical to consider the properties of individual clouds, because these may change rapidly in time. It is more practical and natural to consider properties of *ensembles* of clouds, e.g. cloud systems, or the clouds over a certain area. For cloud ensembles we expect that changes in their intrinsic properties do not take place so rapidly, so that the statistical properties of clouds are easier to establish. Determining these properties requires a network of cloud observation sites over a sufficiently large area, which has led to the choice of the TEBEX network, which will be discussed in Sect. 3.1.1.

For cloud ensembles we should consider *distribution functions* of the above listed individual cloud properties over a certain area. A distribution function of cloud property a over this area, written as $p(a)$, gives the probability of occurrence of a specific value for property a. These distribution functions will generally be altitude- and time-dependent, so they will have the form $p(a, z, t)$. Another way of writing down these distribution functions is by choosing certain altitude layers, e.g. model layers, and taking for each layer i a

distribution function $p(a_i, t)$. For example, the general form of the distribution of the surface areas of clouds in layer i above the TEBEX area at some moment t is $p(A_i, t)$. To first order approximation, this distribution can be represented by the average $\overline{A_i}(t)$ and the standard deviation $\delta A_i(t)$. Division of $\overline{A_i}(t)$ by the TEBEX surface area, yields the fractional cloud cover in layer i over the TEBEX area, denoted by $C_i(t)$. Also the time averages (over some standard period) of these quantities will be needed, which are denoted by $\langle\overline{A_i}\rangle$, $\langle\delta A_i\rangle$, and $\langle C_i\rangle$.

The above mentioned cloud parameters are listed in approximate order of importance. In Sect. 4 we will discuss which of these cloud parameters can be observed in practice with the available instruments, to be discussed in Sect. 3.

2.2 Radiation parameters

The relevant parameters of atmospheric radiation are:

(a) SW flux, spectrally integrated from $\lambda = 0.2$ to 4 μm, throughout the atmosphere (for any z-value):
- downward SW flux $S^{\downarrow}(z)$
- upward SW flux $S^{\uparrow}(z)$
- net SW flux (net = downward - upward) $S(z)$.

(b) LW flux, spectrally integrated from $\lambda = 4$ to 100 μm, throughout the atmosphere:
- downward LW flux $F^{\downarrow}(z)$
- upward LW flux $F^{\uparrow}(z)$
- net LW flux $F(z)$.

(c) Total net flux = net SW flux + net LW flux: $Q(z) = S(z) + F(z)$.
(d) Solar flux incident at TOA: $\mu_0 S_0$, where S_0 is the incident solar flux measured perpendicular to the solar beam. For the average Earth-Sun distance $S_0 = 1370$ W/m^2.
(e) Direct and diffuse components of the downward SW flux at the surface:
- direct component (i.e., attenuated solar flux) $S^{\downarrow}_{\rm dir}(z = 0)$
- diffuse component (i.e., scattered flux) $S^{\downarrow}_{\rm dif}(z = 0)$.

The sum of the direct and diffuse components is $S^{\downarrow}(z = 0)$, which is also called the global radiation.
(f) Spectral SW flux: $S^{\downarrow}(\lambda)$, $S^{\uparrow}(\lambda)$, and $S(\lambda)$, at, e.g., $z = 0$ and TOA.
(g) Spectral LW flux: $F^{\downarrow}(\lambda)$, $F^{\uparrow}(\lambda)$, and $F(\lambda)$, at, e.g., $z = 0$ and TOA.

The spectrally integrated SW and LW fluxes mentioned above are the energetically relevant radiative fluxes, which yield the radiative forcing of the atmosphere. Therefore, these should be measured for TEBEX if possible. In addition, spectral flux measurements can be important, because clouds will also affect the shape of the SW and LW spectrum.

3. Available ground and satellite instruments

In this section a description of the ground and satellite instruments available for TEBEX cloud and radiation observations is given[5]. It is also mentioned which data are stored.

3.1 Ground instruments

3.1.1 Cloud detection network (CDN)

The CDN is a network of lidars (or ceilometers), which can measure the cloud base altitude, and infrared radiometers, which can measure the cloud base temperature. The 10 sites of the CDN are mainly civil and military (KLu) airports in the Netherlands. They cover a central area of about 130×130 km^2 around the Cabauw tower. A larger area of about 200×200 km^2 is covered when 6 extra sites (which only have a lidar) are included. In Fig. 3 the ground sites are shown. In Table 1 they are listed together with the radiation sites (to be discussed later). At the CDN sites the following instruments are or will be installed:

lidar

- Laser operating at $\lambda = 904$–911 nm.
- Type: Vaisala (at KLu sites) or Impulsphysik (at other sites).
- Beam width: 1–2.5 mrad.
- Laser repetition rate: 2.5 kHz.
- Energy per pulse: 1–6.5 $\times$ 10^{-6} J.
- Measured quantity: cloud base altitude and backscatter profile.
- Can measure up to 4 km altitude, with a frequency of 1/30 Hz.
- Located at 10 sites in the central area, and at 6 extra sites in the larger area.
- Stored data: backscatter profile every 30 s (Impulsphysik) or 60 s (Vaisala) for sites in the central area. For sites in the larger area only the cloud base altitude is stored once every 10 min.

infrared radiometer

- Passive radiometer looking at the zenith.
- Operates in the thermal infrared window in a band from $\lambda = 9.6$ to 11.5 μm.
- Field-of-view (FOV): 50 mrad.
- Type: Heimann.
- Measured quantity: brightness temperature between -50°C and $+50$°C, accuracy $\pm$ 0.5° C, response time 3 s.
- Located at 12 sites in the central area.

[5]The instrumentation has been described according to the situation on 1 January 1994; it may be subject to small changes in the future

- Stored data: average, minimum, maximum, number of measurements in a certain band around the minimum and number of measurements in a certain band around the maximum, for 10-min. periods.
Also stored are the occurrences of precipitation (then the protective shutter closes).

As an illustration of the type of data obtained with the CDN instruments, an example of lidar measurements is given in Fig. 4 and of Heimann radiometer measurements in Fig. 5. These data sets have been taken simultaneously on 20 June 1993. From these figures it can be seen, for example, that a broken cloud system is present above Cabauw from about 0800 UT until about 1700 UT.

In Cabauw a video-camera (color S-VHS system) is installed, which takes an image of the sky every 3.2 s. The FOV is: horizontally 108° × vertically 88°, pointing in the northern direction. In this way the cloud structure development is recorded at one site. This may also help in interpreting the lidar data. An example of a video-image is shown in Fig. 6, for 20 June 1993.

At the National Institute of Public Health and Environmental Protection (RIVM) a lidar system for measuring the boundary layer height is operated. The measured backscatter profiles can also be used for the derivation of the optical extinction coefficient in clouds. This lidar system achieves a much better S/N ratio than the Vaisala or Impulsphysik systems. The RIVM lidar system has the following properties:

RIVM lidar

- Laser operating at λ =1064 nm.
- Type: Home-made.
- Beam width: 0.5 mrad.
- Laser repetition rate: 10 Hz
- Energy per pulse: 7×10^{-2} J.
- Measured quantity: backscatter profiles
- Can measure up to 4 km altitude. Each measurement takes 25 s during which 250 profiles are averaged. Every 4 minutes a measurement is taken.
- Located at Bilthoven.
- Stored data: every 4 minutes a backscatter profile is stored.

At the moment it is under discussion to make some minor adjustments to the lidar system to make it more suitable for the derivation of optical cloud parameters. Thus, the above mentioned specifications are subject to change. Next to this lidar system an infrared radiometer will be installed at the RIVM.

3.1.2 Ground radiation instruments

At all CDN sites plus several other sites (see Table 1), also the global downward SW flux is measured, with the following instrument:

global radiometer

- Upward looking global SW radiometer.
- FOV = 2π sr.
- SW band: 0.3 - 3.0 μm.
- Type: Kipp CM 11 (ventilated).
- Measured quantity: global (=diffuse + direct) downward SW flux.
- Located at 12 sites in the central area, and at 16 sites in the larger area.
- Stored data: average, minimum and maximum of 10-min. periods.

The radiation instruments in Cabauw and Garderen, which are the TEBEX radiation sites, are discussed below.

Cabauw

The following instruments are used at the 2 m level:
- global radiometer (Kipp CM 11, see above)
- global radiometer (Kipp CM 11) equipped with a shadow band to measure only the diffuse SW radiation
- global radiometer (Kipp CM 11) equipped with a shadow sphere of 5° diameter, to measure only the diffuse SW radiation
- direct radiation radiometer (Kipp CH 1 pyrheliometer) with a FOV of 5° around the sun
- downward looking global radiometer (Kipp CM 11) for measuring reflected SW radiation (albedo measurement)
- two longwave radiometers (Eppley) to measure the upward and downward radiation from 3–50 μm
- net radiometer (Fritschen) to measure the net (downward–upward) radiation from 0.3 to 50 μm
- an (upward looking) infrared radiometer (Heimann).
- a downward looking infrared radiometer (Heimann).

Thus, in Cabauw all broad-band SW and LW radiation components at the ground are being measured.

Note that the global radiometers for measuring the diffuse SW radiation miss a part of the diffuse (i.e. scattered) radiation, because the shadow band and the 5° shadow sphere cover

part of the bright aureole around the sun. On the other hand, the direct SW radiation measurement *includes* a part of the aureole, since it uses the same FOV as the shadow sphere. Consequently, the sum of these diffuse and direct radiation measurements should be equal to the global radiation. When interpreting these measurements of direct and diffuse radiation, one should bear in mind that they are, to a certain extent, a mixture of scattered and unscattered sunlight.

At the top of the Cabauw tower (213 m) a global radiometer is installed. A downward looking Heimann radiometer will be placed at about 200 m, to measure the brightness temperature of the ground. With this latter instrument we may, by comparison with the AVHRR brightness temperature in channel 4 (see Sect. 3.2), determine the atmospheric correction in this channel from about 200 m until the top of the atmosphere, for the area around Cabauw.

In addition, the vertical profile of visibility is measured on the Cabauw tower (Wessels, 1984; Monna and Van der Vliet, 1987). However, this measurement is only applicable to fog with a visibility of less than about 500 m.

Garderen

The radiation components in Garderen are being measured 16 m above the tree-tops (which are about 20 m high) by means of the following instruments:
- global radiometer (Kipp CM 11)
- downward looking global radiometer (Kipp CM 11) for measuring reflected SW radiation (albedo measurement)
- two longwave radiometers (Eppley) to measure the upward and downward radiation from 3–50 μm
- net radiometer (Fritschen) to measure the net (downward–upward) radiation from 0.3–50 μm.

Also an upward and a downward looking Heimann are installed, so these measurements may be used to validate satellite measurements of surface brightness temperature.

3.2 Satellite instruments

At KNMI the raw data from the geostationary Meteosat and the polar orbiting NOAA satellites are received continuously (for the Meteosat data, see Muller, 1990; for the NOAA data, see Roozekrans and Prangsma, 1992). While these satellite data are in principle available, the data-processing has still to be set-up to obtain cloud parameters. This will be discussed in Sect. 4.2.

Meteosat

- Operational satellite: Meteosat-4.
- Satellite orbit: geostationary at an altitude of 35800 km above the Earth's surface at 0° latitude and 0° longitude.
- 3 channels:
(1) visible (VIS: 0.5 - 0.9 μm),
(2) water vapour (WV: 5.7 - 7.1 μm),
(3) thermal infrared (IR: 10.5 - 12.5 μm).
- Resolution: for all channels 5×9 km^2 above the Netherlands. In the VIS channel also a twice as high resolution is available, but not (yet) used.
- Images are acquired every 30 min.
- Stored data: partial images of 300 × 200 pixels, which is approximately 1500 × 1500 km^2, between 45° and 60° latitude and between 12°W and 15°E longitude, around the Netherlands.
The raw, unprojected radiances in the VIS, WV and IR channels, for every 30 min. are stored when available. Only the IR and WV radiances are calibrated in flight.
- Reference: Eumetsat (1993), and references in Muller (1990).

AVHRR

- On board the NOAA polar orbiting satellites. Presently NOAA-11 and NOAA-12 are operational.
- Satellite orbit: at about 854 km altitude, with a sun-synchronous orbit; duration about 102 min.
- NOAA-11: overhead at about 0200 LST and 1400 LST.
- NOAA-12: overhead at about 0730 LST and 1930 LST.
- 5 channels:
(1) 0.58 - 0.68 μm (center: 0.63 μm),
(2) 0.725 - 1.1 μm (center: 0.85 μm),
(3) 3.55 - 3.93 μm (center: 3.74 μm),
(4) 10.3 - 11.3 μm (center: 10.8 μm),
(5) 11.5 - 12.5 μm (center: 12.0 μm).
- Resolution: 1.1×1.1 km^2 subsatellite.
- Each of the two NOAA satellites passes the Netherlands two or three times a day, and the HRPT data are received at KNMI.
- Stored data: partial images of approximately 350 × 550 km^2, between 50° and 55° latitude and between 3°E and 8°E longitude, around the Netherlands, including the TEBEX area.
The stored data are the raw, unprojected radiances of all channels and overpasses. Only the radiances of channels 4 and 5 are calibrated in flight.
- References: Schwalb (1978, 1982), Kidwell (1986).

TOVS

- TOVS consists of the HIRS-2 and MSU instruments.
- On board the NOAA polar orbiting satellites.
- HIRS-2 has 19 infrared channels and 1 visible channel, chosen to sound the atmospheric temperature and humidity profile. MSU has 4 microwave channels, chosen for the same purpose.
- Resolution: for HIRS-2 the subsatellite diameter of the FOV is 17.4 km; for MSU this is 6 times as large.
- TOVS data are received, processed and archived at KNMI (see also Sect. 4.2.3).
- Stored data: level 1B radiances (calibrated and Earth-located radiances).
Amount of stored data: 1 Mb per day.
- Reference: Werbowetzki (1981).

As an illustration of the available satellite data for TEBEX, Figs. 7 and 8 show Meteosat and AVHRR images, respectively, for the same day as the ground data shown in Figs. 4–6.

Although the satellite measurements mentioned above are all radiation measurements, these measurements cannot easily be transformed in the required SW and LW *broad-band radiative fluxes* at TOA. There are four main reasons:
(1) The satellite instruments have a narrow FOV, so they measure a radiance (if one may assume that the radiation is isotropic in the FOV). This radiance must be transformed to a flux by integration over all (2π sr) directions of exitance at TOA.
(2) The satellite instruments measure in certain wavelength bands, which do not include the entire SW or LW wavelength range. Therefore, these channel radiances must be transformed to broad-band SW and LW radiances.
(3) In the case of the NOAA satellite instruments, the measurements pertain to fixed times of the day. Since the radiation budget has a strong diurnal variation, these satellite measurements have only limited value.
(4) Furthermore, the visible channels of Meteosat and AVHRR are not absolutely calibrated; only a preflight calibration is available, or sometimes results from calibration campaigns. Therefore, only a relative visible reflectance is obtained in these channels. The thermal infrared channels *are* calibrated (on board or in flight). A good discussion of calibrations of all AVHRR channels and their uncertainties, as relevant to the ARM project, is given in DOE (1993).

What is needed are ERBE-type radiation budget measurements at TOA. The full ERBE satellite experiment lasted only from 1985 to 1988 (cf. Feijt, 1992). We note that the ScaRaB instrument, also designed for measuring radiation budget components, is planned

to be launched end of 1993. For the TEBEX project we have chosen to use the satellite instruments that are presently available, which are mentioned above. In Sect. 5 we will discuss this topic in more detail.

3.3 Auxiliary data on clouds and radiation

Apart from the above mentioned ground and satellite data specially gathered for TEBEX, there are cloud and radiation data routinely gathered every hour in De Bilt and 14 other synop stations in the Netherlands:
- precipitation
- visibility
- global radiation
- duration of sunshine
- visual observations of cloud cover, altitude and type.

In addition, precipitation is measured at many other sites. All these items are stored in the climatological database of KNMI.

Furthermore, there are radar data of precipitating clouds over the TEBEX area from weather radars located at De Bilt and Schiphol; data are available every 15 min.

Also the data from the 6-hourly radiosonde ascents in De Bilt are available. By combining the radiosonde temperature and humidity profile with ground and satellite cloud observations, more information on cloud structure can be derived (see Sect. 4).

3.4 Data archive

An important element of TEBEX will be its data archive. Here the archived data on clouds and radiation are listed.

(a) *Ground data.*
The archived data from the ground instruments mentioned in Sect. 3.1 are tabulated in Tables 2a–b.

(b) *Satellite data.*
- Meteosat data, as described in Sect. 3.2, are being archived from 1 January 1993 onwards.
- AVHRR data, as described in Sect. 3.2, are being archived from 8 March 1993 onwards.
- TOVS data, as described in Sect. 3.2, are being archived, with some interruptions, from 1 December 1991 onwards.

(c) *Ancillary data.*
For the analysis of TEBEX measurements, we can access ancillary databases available at KNMI, such as:
- De Bilt radiosonde data (6-hourly)
- HIRLAM model analyses (3-hourly)
- the climatological database.

4. Observable and derivable cloud parameters

In this section we will describe the cloud parameters that can be observed with the instruments described in Sect. 3 as well as the parameters that can be derived from them.

4.1 Cloud parameters from ground data

Here we consider which of the cloud parameters listed in Sect. 2 are or may become available from the cloud detection network, and briefly mention the method of observation or derivation.

(a) *Geometric properties*

– **cloud base height** z_b: directly observable by the ceilometer.
The cloud base height is produced every 30 s or 60 s by the data processing software of the ceilometers in the central TEBEX area, using the backscatter profile. The cloud base height must be smaller than the maximum range-of-detection (MROD), also produced by the ceilometer software. For clear skies MROD $\approx$ 4 km. This means that high clouds (cirrus) and some mid-level clouds (altocumulus and altostratus at 4–6 km) cannot be detected by the ceilometers.

– **cloud size** in the direction of motion of the cloud base (i.e. the wind direction), d_{mot}:
(1) Derivable from the ceilometer signal if the horizontal velocity of the cloud base is known. This velocity may be derived from the radiosonde windprofile in De Bilt, from the future windprofiler at Cabauw (for altitudes below $\approx$ 2 km), or from the HIRLAM model analysis.
(2) Information on d_{mot} is also derivable from the Heimann signal, provided that the horizontal velocity of the cloud base is known, since the time fraction of cloudy and clear sky is included in the Heimann data per 10-min. period. Note, however, that the Heimann has a larger FOV than the ceilometer, so their values of d_{mot} may differ. This difference may be corrected for using some a priori information on the cloud size distribution.

– **cloud thickness** h: derivable from the ceilometer profiles for optically thin clouds (optical thickness less than 1) at the lidar wavelength (about 908 nm), because for thin clouds not only the base but also the top of the cloud can be seen in the backscatter profiles.

– **cloud cover** over the entire TEBEX area at one specific time, $C(t)$: directly observable under the assumption that the network sites are randomly distributed under the cloud field over the TEBEX area.
Because the network sites are not equidistant and there is an effect from the actual cloud

motion direction over the sites (e.g. cloud streets), this assumption is not generally true. Therefore, effects of cloud distribution and wind direction have to be accounted for in determining cloud cover.

(b) *Macrophysical radiative properties*

- **emissivity** ϵ: derivable from the Heimann brightness temperature under the assumption that the atmospheric temperature correction (see below) as well as the actual cloud base temperature are known (e.g. from a radiosonde profile).

- **optical thickness** τ_0: derivable in some cases.
(1) The lidar backscatter profiles (especially from the RIVM lidar) may be used to retrieve the extinction coefficient of the lower part of the cloud, assuming a value for the backscatter efficiency of the cloud particles. If the cloud geometric thickness h is known, and we may assume that the cloud is homogeneous, τ_0 is found.
(2) For optically thin clouds the extinction profile through the cloud, and thus τ_0, follows from the backscatter profile, again assuming a value for the backscatter efficiency of the cloud particles.
(3) Derivable from the global radiation measurement under the assumption that the sky is fully overcast, and using a radiative transfer model for cloud SW transmission.

(c) *Other macrophysical properties*

- **cloud base temperature** T_b: directly observable from the Heimann.
The infrared radiometer determines the apparent cloud base brightness temperature. The actual cloud base brightness temperature can be determined when the atmospheric influence is known and the emissivity of the cloud base is known or can be assumed. The emissivity of a thick cloud in the Heimann spectral range can be assumed to be one (black body assumption). The atmospheric correction can be performed if the atmospheric temperature and humidity profiles are known, e.g. from a radiosonde measurement[6], by using radiative transfer calculations from Lowtran-7 (Kneizys et al., 1988).

The interdependency of the three parameters: cloud base (or cloud top) brightness temperature, atmospheric correction and cloud base (or cloud top) emissivity is further discussed in Appendix B.

[6]In addition, from mid-1994 onwards the RASS will measure the virtual temperature profile in Cabauw up to about 1 km height.

– **liquid water path** W: derivable from τ_0 assuming an average cloud particle size. The following simple parameterisation may be used (Stephens, 1978):

$$W \approx \frac{2}{3}\,\tau_0\, r_e, \tag{1}$$

where r_e is the effective particle radius in μm and W is in g/m^2. So, assuming a value for r_e for a certain cloud type, W follows from the optical thickness (see also the graphs in Stephens, 1978, 1984, showing W as a function of τ_0 for various cloud types).
Furthermore, a relation similar to another parameterisation of Stephens (1978) may be used, which relates W to the so-called downward effective emissivity of the cloud, $\epsilon_\downarrow$:

$$\epsilon_\downarrow = 1 - \exp(-a_0 W), \tag{2}$$

where a_0 = 0.158 and 0.116 m^2/g for the total and window region of the spectrum, respectively. This method for deriving W has yet to be investigated.

(d) *Microphysical properties*

– **particle number density** n: derivable from the backscatter profiles for the lower part of the cloud, assuming a particle backscatter efficiency.

4.2 Cloud parameters from satellite data

To find the cloud parameters needed for TEBEX from satellite images (i.e., radiances in an instrument grid) we first need a *cloud detection* method which determines whether a pixel is clear, fully cloudy, or partially cloudy. Secondly, a *cloud classification* (or analysis) method is needed, which interpretes the radiances still further, in terms of cloud top height, cloud optical thickness, etc.. These detection and classification methods depend on the instrument used, because of the channel characteristics, viewing angle, etc.. One may distinguish between *threshold methods*, which are performed on individual pixels, and *statistical methods*, which are performed on ensembles of pixels. An example of the latter category is the spatial coherence method of Coakley and Bretherton (1982). Many methods are a mixture of these two categories and are called *hybrid methods*. A review of cloud detection methods was given by Rossow et al. (1985). A more general review on satellite cloud studies was given by Rossow (1989).

One of the problems with satellite cloud detection is the dependency of cloud cover on instrument resolution. Wielicki and Parker (1992) used 30 m resolution Landsat data to assess the influence of degrading the resolution on the retrieved cloud cover. They found that cloud detection algorithms are sensitive to sensor resolution and assumptions about cloud optical thickness. The cloud cover may differ from 0.05 to 0.3 among various cloud detection methods. The resolution dependency was found to be large for pixels of 1 km

and larger. Another problem of satellite images is the accurate *positioning* of the satellite pixels in geographic coordinates.

We will discuss the above topics for the three satellite instruments (Meteosat, AVHRR, and TOVS) separately, and indicate which cloud parameters can be determined.

4.2.1 Meteosat

Cloud detection algorithm

For cloud detection in Meteosat images a bispectral dynamical threshold method based on the ISCCP algorithm (Rossow et al., 1985) has been chosen. In this method spatial and temporal variations of pixel radiances are used for identification of clouds. The often used dynamical-clustering-algorithm (Desbois and Sèze, 1984) is inappropriate, because its interpretation in terms of cloud and surface type is not easy. We note that effectively we only have the VIS and IR Meteosat channels available for cloud detection, because the WV channel of Meteosat saturates in the lower troposphere. Therefore, the WV channel is only useful for detection of high clouds.

Positioning and processing

The geographic positioning of the Meteosat pixels is performed by ESOC and is available at KNMI. A method for processing the raw Meteosat data is discussed by Muller (1990) and Muller et al. (1990). Assuming that this processing has produced calibrated, geo-located radiances, the following steps in subsequent analysis should be performed:
(1) Normalisation of the VIS radiance by the solar insolation at TOA, so derivation of reflectivity. More simply, a normalisation to perpendicular solar incidence can be performed, so the image is corrected for the variation of solar zenith angle from pixel to pixel.
(2) Correction of the IR radiance for atmospheric influence (see Appendix B).
(3) Projection of the pixels onto another grid, according to the comparison to be made. For quantitative comparison with NOAA data the fixed Meteosat grid may be most useful.

Cloud parameters

The following cloud parameters can in principle be determined from the planned cloud detection and analysis for the Meteosat images.

(a) *Geometric properties*

– horizontal **size**, **shape**, and **surface area**: observable in the projected instrument grid,

with the resolution of 5 km (lon) by 9 km (lat). The procedure is to count connected cloudy pixels.
Since the TEBEX area is inclined with an angle of 52° towards the Meteosat image plane, the cloud size and shape are 52° projections, relative to the horizontal plane. Transforming back we can obtain the horizontal cloud size and area parameters d_x, d_y and A.

- **cloud cover** C over the entire TEBEX area at every 30 min.: follows directly from the above parameters.

- **cloud top height** z_t: derivable from the cloud top temperature (see below) and the temperature profile (from radiosonde, TOVS, or HIRLAM analysis data).

- **cloud size** in the direction of motion of the cloud base, d_{mot}, which is measured by the CDN, can also be derived from the satellite images if they are scanned in the direction of the cloud base motion.

(b) *Macrophysical radiative properties*

- **(bidirectional) reflectivity** R: observable for the VIS channel, assuming that an absolute calibration is available. The calibrated reflectivity is needed for, e.g., determining the optical thickness of clouds, and long-term trend analysis of cloud properties. Visual calibration coefficients may be taken from the literature (Kriebel and Amann, 1990; Brest and Rossow, 1992).

- **albedo** ρ: derivable from the reflectivity R in the VIS channel, if the anisotropy of the reflected radiation can be assessed. The anisotropy functions (also called limb-darkening functions) that are used in ERBE data processing might be employed (cf. Feijt, 1992, and references therein), or the results from radiative transfer calculations for various types of clear and cloudy atmospheres, e.g. the results shown in Fig. 9.

- **absorption** α: derivable from the albedo ρ if the transmission τ and the surface albedo are known.
The transmission may be found from ground measurements of global radiation, and the surface albedo can be estimated or taken from ground data. The absorption is an important quantity, because it represents the SW heating in the cloud. However, since the absorption is measured as a small difference of two large quantities, its uncertainty will be large.

- **emissivity** ϵ: the deviation of a cloud from a black body (i.e. the deviation of ϵ from 1) may be found from the calibrated IR radiance if we know the actual cloud top temperature (e.g. from a radiosonde profile), the surface temperature, and the atmospheric influence

on the IR radiance (see Appendix B). According to Stephens (1978) clouds do not achieve black body characteristics when their liquid water paths are less than about 30 g/m^2.

– **optical thickness** τ_0: derivable from the calibrated reflectivity in the VIS channel. This derivation needs a radiative transfer model to simulate cloud reflectivity. Such a model usually assumes plane-parallel clouds and certain single scattering properties for the cloud particles (single scattering albedo and scattering function). A radiative transfer method that can take into account multiple scattering by clouds in an exact manner is the doubling/adding method (Van de Hulst, 1980). This method has been implemented for UV-visible radiation in the Earth's atmosphere by Stammes (1993), and is called the DAK model. Fig. 9 shows the reflectivity at TOA for $\lambda = 0.6$ μm, computed by the DAK model, as a function of the cloud optical thickness, for various geometries relevant to Meteosat. These (or similar) curves can be used to derive the cloud optical thickness from the observed reflectivity for a certain geometry Sun-Earth-satellite.

We note that the macrophysical radiative properties of clouds determined from satellite data, as discussed above, will often relate to ensembles of clouds, because of lack of spatial resolution of the satellite instruments. This should be borne in mind when interpreting these properties with models which simulate the radiative properties of individual clouds or plane-parallel cloud layers.

(c) *Other macrophysical properties*

– **liquid water path** W: derivable from τ_0, using the parameterisation of Eq. (1), and assuming an average cloud particle size. Also the IR emissivity parameterisation of Stephens (1978), Eq. (2), can be used to find an estimate for W. For the case of satellite observations $\epsilon_\downarrow$ becomes $\epsilon_\uparrow$, and $a_0 = 0.130$ m^2/g for the total spectrum.
– **cloud top temperature** T_t: follows from the IR radiances, if the emissivity of the cloud top and the atmospheric influence are known or can be assumed. The emissivity of a thick cloud in the IR channel is assumed to be one (black body assumption). For atmospheric correction see Appendix B.

4.2.2 AVHRR

Cloud detection algorithm

There are several algorithms for AVHRR cloud detection. An automated cloud detection and classification method for AVHRR images is the SMHI method (Karlsson and Liljas, 1990), which is a threshold algorithm. Another cloud detection and classification method is the version of the maximum-likelihood method (a statistical method) developed by Berger (1992). This method primarily aims at finding the properties of high clouds.

We will use the hybrid cloud detection method of Saunders and Kriebel (1988), which is known as APOLLO. This method performs well for Europe. Retrievals of cloud properties from AVHRR measurements are possible as well (e.g., Kriebel et al., 1989). The cloud properties that the APOLLO algorithm can yield for cloudy pixels are (from Schickel et al., 1992):
- cloud top temperature
- optical thickness
- liquid water/ice path
- emissivity
- cloud coverage
- cloud type (low, medium, high, ice).

We further note that the AVHRR images that are archived for TEBEX have the size of two ISCCP grid boxes. This is advantageous for future comparison of TEBEX cloud detection results with ISCCP results.

Positioning

The geographic positioning of the AVHRR pixels is performed by the operational AVHRR data reception software (VCS) at KNMI, extended with an interpolation scheme. At the moment the positioning error is $\pm$ 4–5 pixels. This looks like a big problem for combination of AVHRR with ground data, because the aim is to study the same clouds from ground and satellite. The positioning can be improved by applying reference points, but this is not done automatically. An additional, but small, inaccuracy is introduced by the fact that the AVHRR image of the TEBEX area is not truly synoptic. The NOAA satellite moves with about 6.7 km/s relative to the Earth's surface, so the AVHRR instrument scans the TEBEX area in about 20 s. If the windspeed would be 10 m/s, the clouds would move 200 m, i.e. 1/5 of a pixel, during the scan.

However, the positioning accuracy and spatial resolution of the satellite images must be related to the time resolution of the ground observations. Since the TEBEX aim is to study the properties of cloud *ensembles* from ground and space, a satellite positioning inaccuracy of about 5 km is allowed (see also Sect. 6).

Cloud parameters

Generally, most cloud parameters can be determined from (calibrated) AVHRR radiances using procedures analogous to those mentioned above for the Meteosat VIS and IR radiances. However, the lower temporal resolution, higher spatial resolution, and the availability of more channels for AVHRR lead to various differences in the cloud retrieval procedures. We mention a few:
(1) The diurnal variation of cloud properties cannot be monitored well with AVHRR,

because only 4 overpasses from the two NOAA satellites are available at fixed times each day.
(2) The high spatial resolution of AVHRR, however, is well suited for studying geometric and radiative properties of clouds. By comparison with co-located Meteosat data we can validate the cloud detection of the Meteosat images.
(3) The AVHRR cloud images do not suffer from projection problems to the extent as was discussed for Meteosat. This also improves their capability for studying cloud geometric properties.
(4) The availability of 5 AVHRR channels makes it possible to detect various other cloud parameters:
- *Fog* can be detected in day- and night-time AVHRR images by using channels 3 and 4 (Bendix and Bachmann, 1991).
- *Microphysical properties:* Arking and Childs (1985) describe a method based on radiative transfer theory to derive a microphysical parameter, m, from the channel 3 radiances, assuming that the cloud optical thickness, cloud top temperature and the cloud cover fraction of a pixel are determined from the other channels. The parameter m is a combination of cloud particle size and phase[7]. Recently, Platnick and Twomey (1992) have shown results of using the channel 3 radiance for deriving cloud drop size.
The principle behind these methods is that liquid water (and ice) have varying absorption properties in the SW region of the spectrum. In the visible clouds are nonabsorbing. There their reflectivity is mainly determined by their optical thickness. In the near-IR water has several absorption bands (at 0.94, 1.65, 2.16 and 3.7 μm). There cloud reflectivity is mainly determined by the cloud particle radius. This holds for optically thick clouds ($\tau_0 \gtrsim 9$; see Nakajima and King, 1990).
The different absorption properties of ice at 11 and 12 μm may also be exploited to derive the cirrus particle size from the channel 4 and 5 brightness temperatures of cirrus clouds (Parol et al., 1991). Prangsma and Roozekrans (1986) have described a method to detect thin cirrus clouds using channel 4 and 5 brightness temperatures.

Apart from the positioning inaccuracy discussed above, major error sources for the use of AVHRR radiances are:
(1) *Calibration of channels 1 and 2.*
Generally, one uses tables of pre-flight calibration coefficients published by NOAA, as is done e.g. by Karlsson and Liljas (1990). Unfortunately, recent studies have shown that the calibration of the visible channels can change significantly from the pre-launch values (up to 25 %) and that the calibration can drift over time (up to 7 %/year). Therefore, indirect calibration methods using specific reflection targets on the Earth's surface, e.g. desert or ocean glint, are being applied (for an overview, see Thorne and Vitko in DOE, 1993).

[7]Regarding microphysical cloud properties, such as particle size and shape, the use of polarisation data is advantageous. This can only be exploited when polarisation observation satellite instruments, like POLDER and also GOME, become available in the future (respectively in 1996 and 1995).

Most recently, Kaufman and Holben (1993) published calibration coefficients for AVHRR until 1990. Berger (1992) employs manually selected pixels with a known reflectivity (the sea surface as a dark pixel and a thick convective cloud as a bright pixel), to calibrate the channel 1 and 2 images.

2. *Atmospheric correction of channels 1 and 2.*

This is probably not such a big problem in normal situations when the stratospheric and upper tropospheric aerosol content is low; then, if neccessary, the background aerosol optical thickness can be used, and a radiative transfer model can compute the correction factor. However, when the aerosol loading is large due to a volcanic outbreak this is more of a problem. Also when haze layers are present above low clouds cloud detection becomes more ambiguous.

4.2.3 TOVS

The TOVS data-processing at KNMI is based on the 3I inversion method from LMD (cf. Chédin et al., 1985; Roozekrans and Prangsma, 1992). The available 3I TOVS products that are relevant for TEBEX are (LMD, 1989):

- temperature and humidity profiles
- brightness temperatures in HIRS-2 window channels (8, 18 and 19) corrected for water vapour absorption and emissivity
- effective cloud amount
- cloud top pressure
- cloud top temperature.

At the moment these quantities are only available for large boxes of 100 × 100 km^2. The original cloud detection algorithm within the 3I method is discussed by Wahiche et al. (1985). A disadvantage of TOVS for cloud information is its low spatial resolution. It seems possible, however, to produce the above listed quantities also for each HIRS-2 spot, i.e. with a resolution of 30 × 30 km^2, which would be more useful for TEBEX. This extension of 3I could be provided in the framework of the AVHRR/TOVS EC-project (see below). Furthermore, the HIRS-2 channels contain several valuable pieces of information for cloud studies:

(1) The actual atmospheric temperature profile from TOVS leads to a better cloud top altitude determination for the AVHRR data.

(2) The H_2O channel radiances provide information on the humidity profile, so we can derive the water vapour content of the atmosphere (see for a recent discussion of the use of TOVS data for water vapour column determination, Bates and Stephens, 1991).

(3) Using the HIRS-2 CO_2 channels it is possible to detect the presence and altitude of cirrus clouds. This is called the CO_2 slicing technique (for recent discussions, see e.g. Wylie and Menzel, 1991, and Baum and Wielicki, 1992).

Fig. 10 shows an example of a KNMI TOVS-3I product, namely the water vapour column

(in mm) for a NOAA-11 orbit on 20 June 1993.

A combination of TOVS and AVHRR data would be a powerful tool for cloud studies, because the TOVS profiles can lead to better cloud top altitudes, while the AVHRR data provide high resolution imaging in the horizontal plane. An EC-project proposal on this subject, with one of us (G.J.P.) as coordinator, was recently approved. The problem of co-locating TOVS and AVHRR pixels is also part of the EC-project.

5. Observable and derivable radiation parameters

5.1 Radiation parameters from ground data

The vertical profiles of the net SW flux S and net LW flux F, which have been mentioned in Sect. 2.2 and are needed to find the radiative heating rate of the atmosphere, can only be measured in TEBEX at the surface and, with some assumptions, at TOA (see below). A radiative transfer model would be needed to determine the profiles of S and F, given the boundary values. In the following, we will distinguish between the radiation parameters that can be derived from the extensive radiation data acquired at Cabauw and Garderen, and the parameters that can be derived from the limited radiation measurements at the other (CDN) sites.

Cabauw and Garderen

The observed radiative fluxes in Cabauw at ground level are (cf. Sect. 3.1.2):
- the **downward SW flux** $S^{\downarrow}(z = 0)$
- the **direct SW flux** $S^{\downarrow}_{\mathrm{dir}}(z = 0)$
- the **diffuse downward SW flux** $S^{\downarrow}_{\mathrm{dif}}(z = 0)$
- the **upward SW flux** $S^{\uparrow}(z = 0)$
- the **downward LW flux** $F^{\downarrow}(z = 0)$
- the **upward LW flux** $F^{\uparrow}(z = 0)$
- the **net flux** for the entire spectrum $Q(z = 0)$.

Some consistency checks of these fluxes are possible:
- The relationship $Q = S^{\downarrow} - S^{\uparrow} + F^{\downarrow} - F^{\uparrow}$ can be used as a check of one of these five fluxes.
- The diffuse downward SW flux $S^{\downarrow}_{\mathrm{dif}}(z = 0)$ can be checked by subtracting the direct flux $S^{\downarrow}_{\mathrm{dir}}(z = 0)$ from the global flux $S^{\downarrow}(z = 0)$.

In Garderen $S^{\downarrow}$, $S^{\uparrow}$, $F^{\downarrow}$, $F^{\uparrow}$, and Q are measured at 16 m above the tree-tops.

The above mentioned observed radiative fluxes at the surface of two TEBEX sites can directly be used in TEBEX modelling and parameterisation efforts.

In principle, the global radiation measured at the top of the Cabauw tower may be used in combination with the global radiation at ground level, to estimate the aerosol optical thickness of the lowest 200 m of the atmosphere in Cabauw. Because of the required accuracy, this will probably only work in the case of fog (or low cloud).

Other sites

At the other TEBEX network sites the global SW radiation is the only directly measured radiation parameter. However, some information on the downward LW radiation will be obtained at the CDN sites in the central TEBEX area, because the Heimann radiometer measures the zenith brightness temperature in the atmospheric window. If this zenith radiation can be uniquely related to the downward LW flux by using the data obtained in Cabauw and Garderen, where both quantities are measured, the Heimann data at all CDN sites may be transformed to downward LW fluxes.

From a combination of the radiation parameters measured at the sites in the central TEBEX area with cloud observations (e.g. cloud cover, and distributions of cloud size, cloud base altitude and cloud optical thickness) over the same area, we may derive empirical relations between radiation and cloud parameters for a large area. For example, we may relate the area-averaged radiative fluxes to the cloud distributions functions. These can then be compared with predictions from a radiation model of the atmosphere. Furthermore, the empirical relationship between global radiation and cloud cover as proposed by Holtslag and Van Ulden (1983) can be tested.

We note that, in order to model the surface radiation measurements correctly, it is important to know, apart from the cloud parameters, at least three other parameters, namely: the horizontal and vertical atmospheric *turbidity* due to aerosol, the *water vapour* density profile, and the *ozone* density profile. The reason to need the turbidity is that diffuse radiation due to aerosol scattering may otherwise be misinterpreted as being due to clouds. Water vapour and ozone are the most important absorbers in the SW range; in the LW range water vapour is the most important absorber that has a variable concentration. The horizontal turbidity can be found from the visibility (see Sect. 3), and the vertical turbidity from the RIVM lidar measurements. The water vapour profile can be found from radiosonde measurements in De Bilt and HIRLAM analyses. The ozone column density and ozone profile are measured in De Bilt; if the required accuracy permits, climatological ozone data can be used.

5.2 Radiation parameters from satellite data

As mentioned in Section 3.2, the satellite radiation measurements available for TEBEX radiation studies suffer from several limitations, which are angular, spectral, or temporal in nature. Therefore, we have to apply several correction factors to transform the satellite measurements of narrow-band radiances into broad-band radiative fluxes:
(1) *Angular correction* due to limited FOV and viewing direction.
The anisotropy of the emerging radiation field (SW and LW) at TOA, represented by the anisotropy function R (which is similar to the bidirectional reflectivity defined in Sect.

2.1), must be known to transform the radiance L into a flux M:

$$M = \frac{\pi L}{R}, \tag{3}$$

where L and R depend on the viewing direction, and, in the case of SW radiation, also on the solar direction. R can be estimated from measurements or radiative transfer models. Observed values of the anisotropy functions for the broad-band SW region are given by Suttles et al. (1988), and for the broad-band LW region by Smith et al. (1990). For the SW region, it may also be useful to apply the surface albedo models of Briegleb et al. (1986), which give the surface albedo for various types of surface as a function of solar zenith angle and wavelength.

(2) *Spectral correction* for band width.

A spectral correction factor f_i is needed to transform the flux M_i in some band or channel i of Meteosat (SW: VIS band, LW: IR band) and AVHRR (SW: channels 1 and 2, LW: channels 4 and 5) into a broadband SW flux S or LW flux F:

$$S = f_i M_i \qquad i = \text{VIS, ch. 1, ch. 2} \tag{4}$$

$$F = f_j M_j, \qquad j = \text{IR, ch. 4, ch. 5.} \tag{5}$$

To determine the spectral correction factor one needs a spectral model of clear and cloudy atmospheres. A spectral (low-resolution) radiative transfer model like Lowtran-7 may be used. Laszlo et al. (1988) give conversion factors for estimating broad-band reflectivities from narrow-band reflectivities (see also Pinker and Laszlo, 1992).

(3) *Diurnal variation correction.*

The Meteosat radiation measurements are ideally suited to monitor the diurnal variation of radiation at TOA, provided that one can correct for the fixed viewing angle of Meteosat and the VIS and IR band widths. Schmetz and Liu (1988) describe a method for obtaining the outgoing LW flux at TOA using Meteosat IR and WV channel data (see also Schmetz et al., 1990). A method for estimating the LW flux at TOA from AVHRR data is discussed by Lagouarde et al. (1991).

For climate studies it is important to obtain global data on the SW and LW downward fluxes *at the surface.* These can be derived from satellite measurements, as has been done, e.g., by Schmetz (1991, 1993). At the basis of the method lies a radiative model of the atmosphere. Another way to derive the downward SW flux at the surface from satellite measurements has been described by Pinker and Laszlo (1992). A simple yet accurate parameterisation to obtain the net SW flux at the surface from the reflected flux at TOA, only requiring the water vapour column density and the solar zenith angle, has recently been presented by Li et al. (1993). These algorithms to derive surface fluxes may be tested using the TEBEX database.

6. Combining ground and satellite data

An important task will be the linking up of ground and satellite observations to find the cloud parameters needed, especially the three-dimensional cloud distribution. This topic will only be briefly addressed in this section. We mention the following problems in combining ground and satellite data:
(i) The ground and various satellite parts of the TEBEX cloud observation system have their own spatial and temporal resolutions.
(ii) Since the surface and satellite observations give mainly information on the cloud bases and cloud tops, respectively, the vertical structure, and especially the layering of the clouds, remains largely unobserved.
(iii) The geographic positioning of satellite pixels generally cannot be done more accurately than $\pm$ 2 pixels, i.e. an inaccuracy of $\geq$ 10–20 km for Meteosat images, and $\geq$ 2 km for AVHRR images. The usual inaccuracy of AVHRR is 4–5 km subsatellite. This means that an exact co-location of ground and satellite observations will not be possible, which would be needed to study the same individual cloud from ground and satellite.

However, since the *statistical* properties of cloud fields and not the individual properties of isolated clouds are relevant for TEBEX (cf. Sect. 1), the combination of ground and satellite data becomes less demanding regarding temporal and spatial correspondence. As an example, we consider the ground observations of the radiative fluxes, which are 10-min. characteristics. The corresponding spatial inaccuracy of the ground observations for a cloud system moving with a typical wind speed of 10 m/s is then 6 km. This value agrees well with the usual AVHRR positioning inaccuracy of 4–5 km subsatellite. Concludingly, in this example the ground and satellite observations have similar spatial resolutions, which are not suited for studying the same individual cloud from ground and space, but *are* suited for the same ensemble of clouds.

Apart from being necessary to derive the three-dimensional cloud distribution, the TEBEX cloud observations from ground and space can also be used to validate operational cloud detection schemes for satellite data. This is an important application, especially to study sub-pixel variability of clouds, e.g. the effect of partially cloudy pixels.

As an example of a method to combine ground and satellite observations of clouds we mention the trajectory method, which uses wind vectors for space-to-time conversion of satellite images. The resulting time series of, for example, cloud top temperature can then be compared to time series of, for example, cloud base height observed from ground. This method has been applied by Feijt et al. (1993).

7. Discussion and conclusions

In Sects. 4 and 5 of this report we have discussed various important cloud and radiation parameters that can in principle be determined from the measurements collected in the framework of TEBEX. However, deriving cloud and radiation parameters from measurements usually requires a time-consuming analysis. Therefore, priorities have to be set regarding the parameters which will be analysed for TEBEX. Since the principal application of TEBEX clouds and radiation observations will be to improve parameterisations of clouds and radiation in (regional) climate models, like RACMO, we suggest that the following parameters be derived first:
(a) three-dimensional cloud distribution (cloud cover, cloud top and cloud base height)
(b) cloud top and cloud base temperature distribution
(c) cloud liquid water path distribution
(d) relationship between cloud (or cloud property) distributions and radiative fluxes (SW and LW) at the surface and TOA; more specific: relationship between ensemble properties of clouds and area-averaged radiative fluxes.
The parameters (a)–(c) should be given for the central TEBEX area in statistical terms: average value plus characteristics like standard deviation, minimum, maximum, etc., in standard periods of 30 min. (this is the time resolution of Meteosat). The vertical resolution of the parameters should be as high as possible; the resolution can be degraded for comparison with models (e.g. RACMO).

In addition to the use of TEBEX data for deriving the above parameters and improving the cloud and radiation modules in climate and weather models, various other types of studies will be possible:
1. *Statistical studies* on two years of data, e.g. of the relation between cloud and radiation parameters.
2. *Case studies* of the relation between clouds and radiation, e.g. the relation between cloud characteristics, radiation at the ground, and outgoing radiation at TOA.
3. Study of the effect of cloud inhomogeneity on radiative properties of clouds.
4. Relationship between physical cloud parameters and meteorological cloud type.
5. Verification of clouds as predicted by HIRLAM.

It is now the task of the climate modellers to prepare their models for the use of the large set of observations that will become available in the framework of TEBEX, in order to achieve the aim of improvement of these models.

Acknowledgements

We are grateful to W. Monna and A.P. van Ulden for comments on an earlier version of this report.

References

Arking, A. and J.D. Childs, "Retrieval of cloud cover parameters from multispectral satellite images", J. Clim. Appl. Meteor. **24**, 322–333 (1985)

Bates, J.J. and G.L. Stephens, "Global atmospheric water vapor from satellite data", in: Proc. 6-th Int. TOVS Study Conference, Airlie, 40–49 (1991)

Baum, B.A. and B.A. Wielicki, "On the retrieval and analysis of multilevel clouds", in: Proc. 11-th Conf. on Clouds and Precipitation, Montreal, 1061–1064 (1992)

Bendix, J. and M. Bachmann, "Operational detection of fog in the Alpine region by means of AVHRR imagery of NOAA satellites", Proc. 5-th AVHRR Data Users' Meeting, 307–312, Eumetsat, Darmstadt (1991)

Berger, F.H., "Die Bestimmung des Einflusses von hohen Wolken auf das Strahlungsfeld and auf das Klima durch Analyse von NOAA AVHRR-Daten", Dissertation, Freie Universität Berlin, Reimer, Berlin (1992)

Brest, C.L. and W.B. Rossow, "Radiometric calibration and monitoring of NOAA AVHRR data for ISCCP", Int. J. Rem. Sens. **13**, 235–273 (1992)

Briegleb, B.P., P. Minnis, V. Ramanathan, and E. Harrison, "Comparison of regional clear-sky albedos inferred from satellite observations and model calculations", J. Clim. Appl. Meteor. **25**, 214–226 (1986)

Coakley, J.A., and F.P. Bretherton, "Cloud cover from high-resolution scanner data: detecting and allowing for partially filled fields of view", J. Geophys. Res. **87**, C7, 4917–4932 (1982)

Chédin, A., N.A. Scott, C. Wahiche, and P. Moulinier, "The improved initialization inversion method: a high resolution physical model for temperature retrievals from satellites of the TIROS-N series", J. Clim. Appl. Meteor. **24**, 128–143 (1985)

Desbois, M. and G. Sèze, "Use of space and time sampling to produce representative satellite cloud classifications", Ann. Geophys. **2**, 599–606 (1984)

DOE, "Atmospheric Radiation Measurement Program Plan, Executive Summary", DOE/ER-0442, U.S. Dept. of Energy, Office of Energy Research, Washington DC (1990)

DOE, "The Possible Direct Use of Satellite Radiance Measurements by the Atmospheric Radiation Measurement Program", DOE/ER-0585T, U.S. Dept. of Energy, Office of Energy Research, Washington DC (1993)

Eumetsat, "Directory of Meteorological Satellite Applications", Eds. M.G. Phillips and M. Pooley, BR-03, Eumetsat, Darmstadt (1993)

Feijt, A., "The Earth Radiation Budget Experiment: overview of data-processing and error sources" KNMI Tech. Report TR-146, De Bilt (1992)

Feijt, A., A. van Lammeren, and P. Stammes, "Plans for ground and satellite observations of clouds and radiation in the Netherlands", in: Proc. of the 6-th AVHRR European Data Users' Meeting, 505–511, Eumetsat, Darmstadt (1993)

Kaufman, Y.J., and B.N. Holben, "Calibration of the AVHRR visible and near-IR bands by atmospheric scattering, ocean glint and desert reflection", Int. J. Remote Sensing **14**, 21–52 (1993)

Holtslag, A.A.M. and A.P. van Ulden, "A simple scheme for daytime estimates of the surface fluxes from routine weather data", J. Clim. Appl. Meteor. **22**, 517–529 (1983)

Karlsson, K.-G. and E. Liljas, "The SMHI model for cloud and precipitation analysis from multispectral AVHRR data", SMHI Promis Report Nr. 10, Norrköping (1990)

Kidwell, K.B., "NOAA Polar Orbiter Data Users Guide", U.S. Dept. of Commerce, Washington (1986)

Kneizys, F.X., et al., "Users Guide to LOWTRAN 7", Air Force Geophysics Laboratory, Hanscom AFB (MA), AFGL-TR-88-0177 (1988)

Kriebel, K.T., R.W. Saunders, and G. Gesell, "Optical properties of clouds derived from fully cloudy AVHRR pixels", Beitr. Phys. Atmosph. **62**, 165–171 (1989)

Kriebel, K.T., and V. Amann, "Absolute calibration of the Meteosat-4 VIS-channel", in: Proc. of the 8-th Meteosat Scientific Users' Meeting, 33–38, Eumetsat, Darmstadt (1991)

Lagouarde, J.P., Y. Brunet, Y. Kerr, and J. Imbernon, "Estimating the daily upward longwave radiation from NOAA-AVHRR data for mapping net radiation", Adv. Space Res. **11**, no. 3, 151–161 (1991)

Laszlo, I., H. Jacobowitz, and A. Gruber, "The relative merits of narrowband channels for estimating broadband albedos", J. Atmos. Ocean. Technol. **5**, 757–773 (1988)

Li, Z., H.G. Leighton, and R.D. Cess, "Surface net solar radiation estimated from satellite measurements: comparisons with tower observations", J. Climate **6**, 1764–1772 (1993)

LMD, "3I System User's Guide", Version 08.89, ARA, Laboratoire de Météorologie Dynamique, Paris (1989)

Monna, W.A.A. and J.G. van der Vliet, "Facilities for research and weather observations on the 213 m tower at Cabauw and at remote locations", KNMI Scientific Report WR-87-5, De Bilt (1987)

Muller, S.H., "Quantitative processing of Meteosat data: implementation at KNMI; applications", KNMI Techn. Report TR-127, De Bilt (1990)

Muller, S.H., H. The, W. Kohsiek, and W.A.A. Monna, "Description of Crau data set: Meteosat data, radiosonde data, sea surface temperatures; comparison of Meteosat and Heimann data", KNMI Scientific Report WR-90-03, De Bilt (1990)

Nakajima, T. and M.D. King, "Determination of the optical thickness and effective particle radius of clouds from reflected solar radiation measurements. Part I: Theory", J. Atm. Sci. **47**, 1878–1893 (1990)

Parol, F., J.C. Buriez, G. Brogniez, and Y. Fouquart, "Information content of AVHRR channels 4 and 5 with respect to the effective radius of cirrus cloud particles", J. Appl. Meteor. **30**, 973–984 (1991)

Pinker, R.T. and I. Laszlo, "Modelling surface solar irradiance for satellite applications on a global scale", J. Appl. Meteor. **31**, 194–211 (1992)

Platnick, S. and S. Twomey, "Remote sensing the susceptibility of cloud albedo to changes in drop concentration" in: Proc. 11-th Conf. on Clouds and Precipitation, Montreal, 785–788 (1992)

Pollinger, W., and P. Wendling, "A bispectral method for the height determination of optically thin ice clouds", Beitr. Phys. Atmosph. **57**, 269–281 (1984)

Prangsma, G.J., and J.N. Roozekrans, "Processing of raw digital NOAA-AVHRR data for sea and land applications", in: "Remote Sensing for Resources Development and Environmental Management", Eds. M.C.J. Damen et al., 63–66, Rotterdam (1986)

Roozekrans, J.N. and G.J. Prangsma, "Observatie van het aard-atmosfeersysteem door de NOAA-satellieten", BCRS Report NRSP-1 92-02 (1992)

Rossow, W.B., F. Mosher, E. Kinsella, A. Arking, M. Desbois, E. Harrison, P. Minnis, E. Ruprecht, G. Sèze, C. Simmer, and E. Smith, "ISCCP cloud algorithm intercomparison" J. Clim. Appl. Met. **24**, 877–903 (1985)

Rossow, W.B., "Measuring cloud properties from space", J. Climate **2**, 201–213 (1989)

Saunders, R.W. and K.T. Kriebel, "An improved method for detecting clear sky and cloudy radiances from AVHRR data", Int. J. Remote Sensing **9**, 123–150 (1988)

Schickel, K.P., H.E. Hoffmann, and K.T. Kriebel, "Identification of icing water clouds by NOAA AVHRR satellite data", in: Proc. 11-th Conf. on Clouds and Precipitation, Montreal, 399–400 (1992)

Schiffer, R.A., and W.B. Rossow, "The International Satellite Cloud Climatology Project (ISCCP) – the first project of the World Climate Research Program", Bull. Am. Meteor. Soc. **64**, 779-784 (1983)

Schmetz, J., "An atmospheric-correction scheme for operational application to Meteosat infrared measurements", ESA Journal **10**, 145–159 (1986)

Schmetz, J., "Retrieval of surface radiation fluxes from satellite data", Dyn. Atm. Oceans **16**, 61–72 (1991)

Schmetz, J., "Relationship between solar net radiative fluxes at the top of the atmosphere and at the surface", J. Atmos. Sci. **50**, 1122–1132 (1993)

Schmetz, J., and Q. Liu, "Outgoing longwave radiation and its diurnal variation at regional scales derived from Meteosat", J. Geophys. Res. **93**, D9, 11192–11204 (1988)

Schmetz, J., M. Mhita, and L. van de Berg, "METEOSAT observations of longwave cloud-radiative forcing for April 1985", J. Climate **3**, 784–791 (1990)

Schwalb, A., "The Tiros-N/NOAA A-G Satellite Series", NOAA Tech. Mem. NESS 95, Suitland (MA) (1978)

Schwalb, A., "Modified version of the Tiros-N/NOAA A-G Satellite Series (NOAA E-J) – Advanced Tiros N (ATN)", NOAA Tech. Mem. NESS 116, Washington D.C. (1982)

Smith, G.L., N.D. Manalo, and L.M. Avis, "Limb-darkening functions as derived from along-track operation of the ERBE scanning radiometers for August 1985", NASA Reference Publ. 1243, Washington D.C. (1990)

Stammes, P., "Influence of clouds on radiative flux profiles and polarization", in: "IRS '92: Current problems in atmospheric radiation", Eds. S. Keevallik and O. Kärner, 129–132, A. Deepak, Hampton, VA (1993)

Stephens, G.L., "Radiation profiles in extended water clouds. II: parameterization schemes", J. Atm. Sci. **35**, 2123–2132 (1978)

Stephens, G.L., "The parameterization of radiation for numerical weather prediction and climate models", Mon. Wea. Rev. **112**, 826–867 (1984)

Suttles, J.T., R.N. Green, P. Minnis, G.L. Smith, W.F. Staylor, B.A. Wielicki, I.J. Walker, D.F. Young, V.R. Taylor, and L.L. Stowe, "Angular Radiation Models for Earth-Atmosphere System", NASA Ref. Publ. 1184, Washington D.C. (1988)

van de Hulst, H.C., "Multiple light scattering: tables, formulas and applications", Academic Press, New York (1980)

Wahiche, C., N.A. Scott, and A. Chédin, "Cloud detection and cloud parameters retrieval from the satellites of the TIROS-N series", Ann. Geophys. **4**, 207–222 (1986)

Werbowetzki, A., "Atmospheric Sounding User's Guide", NOAA Tech. Report NESS 83, Washington D.C. (1981)

Wessels, H.R.A., "Cabauw meteorological data tapes 1973–1984; description of instrumentation and data processing for the continuous measurements", KNMI Scient. Report 84-6, De Bilt (1984)

Wielicki, B.A., and L. Parker, "On the determination of cloud cover from satellite sensors: the effect of sensor spatial resolution", J. Geophys. Res. **97**, D12, 12799–12823 (1992)

WMO, "Global Energy and Water Cycle Experiment (GEWEX), Report of the Fourth Session of the JSC Scientific Steering Group", WCRP-74, WMO, Geneva (1992)

Wylie, D., and W.P. Menzel, "Two years of global cirrus cloud statistics using HIRS", in: Proc. of Sixth International TOVS Study Conference, p. 525, Airlie (VA), May 1–6, 1991

Appendix A. List of abbreviations

APOLLO	AVHRR processing over land, cloud and ocean
ARM	Atmospheric Radiation Measurement Program (U.S.A.)
AVHRR	Advanced Very High Resolution Radiometer (NOAA)
CDN	Cloud Detection Network
DAK	Doubling-Adding KNMI
DLR	Deutsche Forschungsanstalt für Luft- und Raumfahrt
EC	European Community
ESA	European Space Agency
ESOC	European Space Operations Centre
EUMETSAT	European Meteorological Satellite (Programme)
FOV	field-of-view
GEWEX	Global Energy and Water Cycle Experiment
GOME	Global Ozone Monitoring Experiment (ESA)
HIRLAM	High Resolution Limited Area Model
HIRS	High Resolution Infrared Sounder
HRPT	High Resolution Picture Transmission
ISCCP	International Satellite Cloud Climatology Project
KLu	Koninklijke Luchtmacht
KNMI	Koninklijk Nederlands Meteorologisch Instituut
LMD	Laboratoire de Meteorologie Dynamique
LST	local solar time
LW	longwave (thermal infrared region of spectrum)
METEOSAT	Meteorological Satellite (EUMETSAT/ESA)
MROD	maximum range of detection
MSU	Microwave Sounding Unit
NOAA	National Oceanic and Atmospheric Administration (U.S.A.)
NOAA-n	series of meteorological polar satellites (NOAA)
POLDER	Polarisation and Directionality of the Earth's Reflectance (France)
RACMO	Regional Atmospheric Climate Model
RASS	Radio Acoustic Sounding System
RIVM	National Institute of Public Health and Environmental Protection
ScaRaB	Scanner for the Radiation Budget
SMHI	Swedish Meteorological and Hydrological Institute
SW	shortwave (solar region of spectrum)
TEBEX	Tropospheric Energy Budget and Water Cycle Experiment
TOA	top-of-the-atmosphere
TOVS	TIROS Operational Vertical Sounder
UT	universal time (= Greenwich mean time)
WCRP	World Climate Research Programme
3I	Improved Initialization Inversion

Appendix B. Atmospheric correction of IR measurements

Measurements of cloud top and cloud base equivalent brightness temperature by means of, respectively, satellite IR channels and Heimann radiometers, have to be corrected for infrared absorption and emission by the atmosphere between cloud top (or base) and detector, in order to obtain the actual cloud top and base temperature. To calculate this correction term one needs a radiative transfer model and the following input parameters:
- atmospheric temperature profile $T(z)$
- atmospheric humidity profile $q(z)$
- surface temperature
- emissivity of cloud top (or base)
- height of cloud top (or base)
- temperature of cloud top (or base)
- viewing angle
- filter characteristics of detector
- aerosol profile.

An operational correction method for Meteosat IR data has been described by Schmetz (1986), which uses ECMWF model forecasts for $T(z)$ and $q(z)$. Another method for Meteosat data has been discussed by Muller (1990) and applied by Muller et al. (1990) for the Crau-experiment.

For TEBEX we plan to use Lowtran-7 (Kneizys et al., 1988) as the radiative transfer model, and to use $T(z)$ and $q(z)$ from either radiosonde measurements, HIRLAM model analyses, or TOVS retrievals. The viewing angle and filter characteristics of the detector are known. For the aerosol profile a background profile will be assumed, unless more information is known (e.g. from the RIVM lidar). The influence of aerosol on the IR correction is usually very small (about 0.1 °C at TOA); only during extreme conditions (e.g. volcanic eruptions) it can be 1–2 °C at TOA (Schmetz, 1986). For the cloud emissivity we will assume a value of 1 as a first approximation. However, this does not hold for e.g. thin cirrus clouds; in that case a bispectral method, using the IR and WV channels, might be applied (cf. Pollinger and Wendling, 1984). Now the unknown quantities are the cloud top (or base) temperature and height. As an initial guess, we will use the measured brightness temperature and the corresponding height according to the temperature profile. Then the atmospheric correction will be calculated with Lowtran-7, and applied to the initial guess temperature to obtain the corrected temperature. This procedure has to be iterated until convergence occurs.

Table 1. Ground network sites of cloud and radiation observations for TEBEX, with available instrumentation. No. is the station number. CDN means that the site belongs to the Cloud Detection Network.

No.	Name	CDN	Lidar (a)	Heimann	Global rad.	Other instruments
210	Valkenburg	yes	A	x	A	
235	De Kooy		A		A	
240	Schiphol	yes	x (b)	x	A	
242	Vlieland		x			
265	Soesterberg	yes	A	x	A	
270	Leeuwarden		x		A	
275	Deelen	yes	A (c)	x	A	
280	Eelde		x (b)		A	
290	Twenthe		x		A	
340	Woensdrecht	yes	A	x		
344	Rotterdam	yes	x (b)	x	A	
348	Cabauw	yes	A	x (↓↓↑)	A	SW (dir., diff.), SW (up) LW (up, down), net
350	Gilze-Rijen	yes	A	x	A	
370	Eindhoven	yes	A	x	A	
375	Volkel	yes	A	x	A	
380	Beek		x (b)		A	
–	Garderen			A (↓↑)	A	SW (up), LW (up, down), net
–	RIVM		A	x		
–	F03		x			
385	De Peel		x (d)		A	

Notes:
All data (except backscatter profiles) are 10-min. data
x = data not yet archived
A = data are being archived from 1 January 1994 onwards (or earlier)
(a) = lidar data at CDN sites includes backscatter profiles
(b) = data acquisition via Luchtvaart Meteorologische Dienst
(c) = from 1 August 1993 onwards
(d) = is not automatic (so not useful for the database).

Table 2a. Quantities in the CDN database. All data relate to 10-min. periods, except when stated otherwise.

Quantity	specification
Global radiation	average, minimum, maximum
Cloud base height	max. 2 cloud layers
IR radiometer temperature	average, minimum, maximum,
	# of points in band around min. and max.
Backscatter profiles Cabauw	30 s data
Backscatter profiles RIVM	original 4 min. data
	aerosol product
	cloud product
SW radiation Cabauw	average, minimum, maximum of:
	$S^{\downarrow}$, $S^{\downarrow}_{dif}$, $S^{\downarrow}_{dir}$, and $S^{\uparrow}$ at 2 m, and $S^{\downarrow}$ at 200 m
LW radiation Cabauw	average, minimum, maximum of $F^{\uparrow}$ and $F^{\downarrow}$ at 2 m
Temperature Cabauw	average T at 0 m
	average T at 2 m
	average T at 200 m
	average wet-bulb T at 2 m
	average wet-bulb T at 200 m
Precipitation Cabauw	sum over 10 min.
Video images Cabauw	every 3.2 s during daytime

Table 2b. Number of datafiles in the CDN database for 1993.

1993 data sheet

Weeknumber	1	2	3	4	5	6	7	8	9	10	11	12	13	14	15	16	17	18	19	20	21	22	23	24	25	26
Shortwave radiation	-	-	-	-	-	-	-	-	-	-	-	-	27	27	27	27	27	27	27	27	27	27	27	27	27	27
IR-radiometers	-	-	-	-	-	-	-	-	-	-	-	-	-	-	-	-	-	-	-	-	-	-	1	1	1	-
10 min cloud base	-	-	-	-	-	-	-	-	-	-	-	-	2	2	2	2	2	2	2	2	2	2	2	2	2	2
Backscatter profiles KLU	-	-	-	-	-	-	-	-	-	-	-	-	-	-	-	-	-	-	-	-	-	-	-	-	-	-
Backscatter profiles airports	-	-	-	-	-	-	-	-	-	-	-	-	-	-	-	-	-	-	-	-	-	-	-	-	-	-
RIVM Lidar	-	-	-	-	-	-	-	-	-	-	-	-	1	1	1	1	1	1	1	1	1	1	1	-	-	-
Cabauw LIDAR	1	1	1	1	1	1	1	1	1	1	1	1	1	1	1	1	1	1	1	1	1	1	1	1	1	1
Cabauw data	-	-	-	-	-	-	-	-	-	-	-	-	4	4	4	4	4	4	4	4	4	4	4	4	4	4
Video	1	1	1	1	1	1	1	1	1	1	1	1	1	1	1	1	1	1	1	1	1	1	1	1	1	1

Weeknumber	27	28	29	30	31	32	33	34	35	36	37	38	39	40	41	42	43	44	45	46	47	48	49	50	51	52
Shortwave radiation	27	27	27	27	29	29	29	30	30	30	30	30	30	30	30	30	30	30	30	30	30	30	30	30	30	30
IR-radiometers	-	-	-	-	1	1	1	-	-	-	-	-	-	-	-	-	-	-	-	1	2	2	2	1	1	1
10 min cloud base	2	2	2	3	3	3	4	4	4	4	4	4	4	4	4	4	4	4	4	4	4	4	4	4	4	5
Backscatter profiles KLU	-	-	-	-	2	2	3	4	4	4	3	3	3	1	2	4	4	2	3	4	6	6	4	5	5	4
Backscatter profiles airports	-	-	-	-	-	-	-	-	-	-	-	-	-	-	-	-	-	-	-	-	-	-	-	-	-	-
RIVM Lidar	1	1	1	1	1	1	1	1	1	1	1	1	1	1	1	1	1	1	1	1	1	1	1	-	-	-
Cabauw LIDAR	1	1	1	1	1	1	1	1	1	1	1	1	1	1	1	1	1	1	1	1	1	1	1	1	1	1
Cabauw data	4	4	4	4	4	4	4	4	4	4	4	4	4	4	4	4	4	4	4	4	4	4	4	4	4	4
Video	1	1	1	1	1	1	1	1	1	1	1	1	1	1	1	1	1	1	1	1	1	1	1	1	1	-

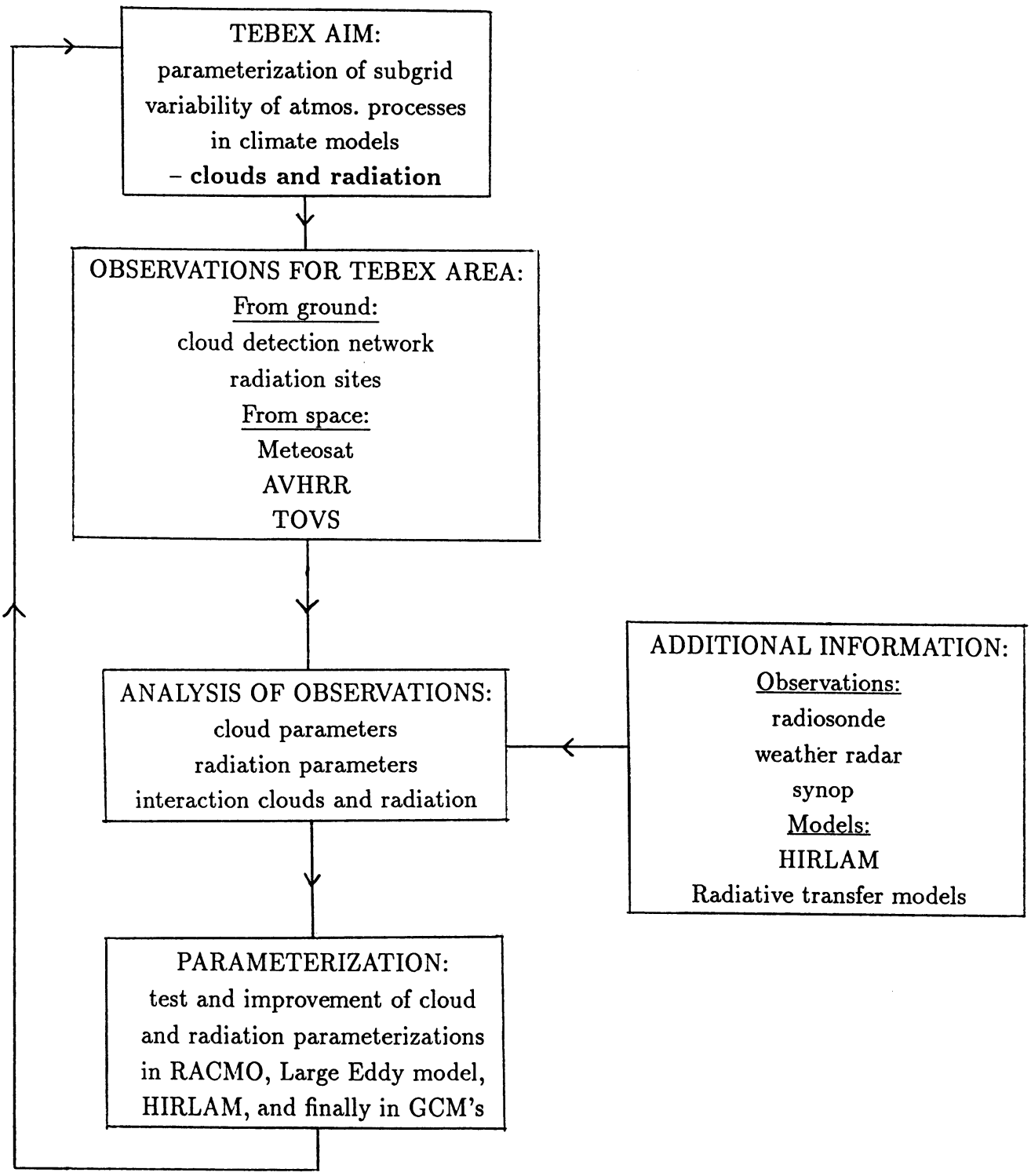

Figure 1. Schematic overview of the elements of TEBEX and their interrelations.

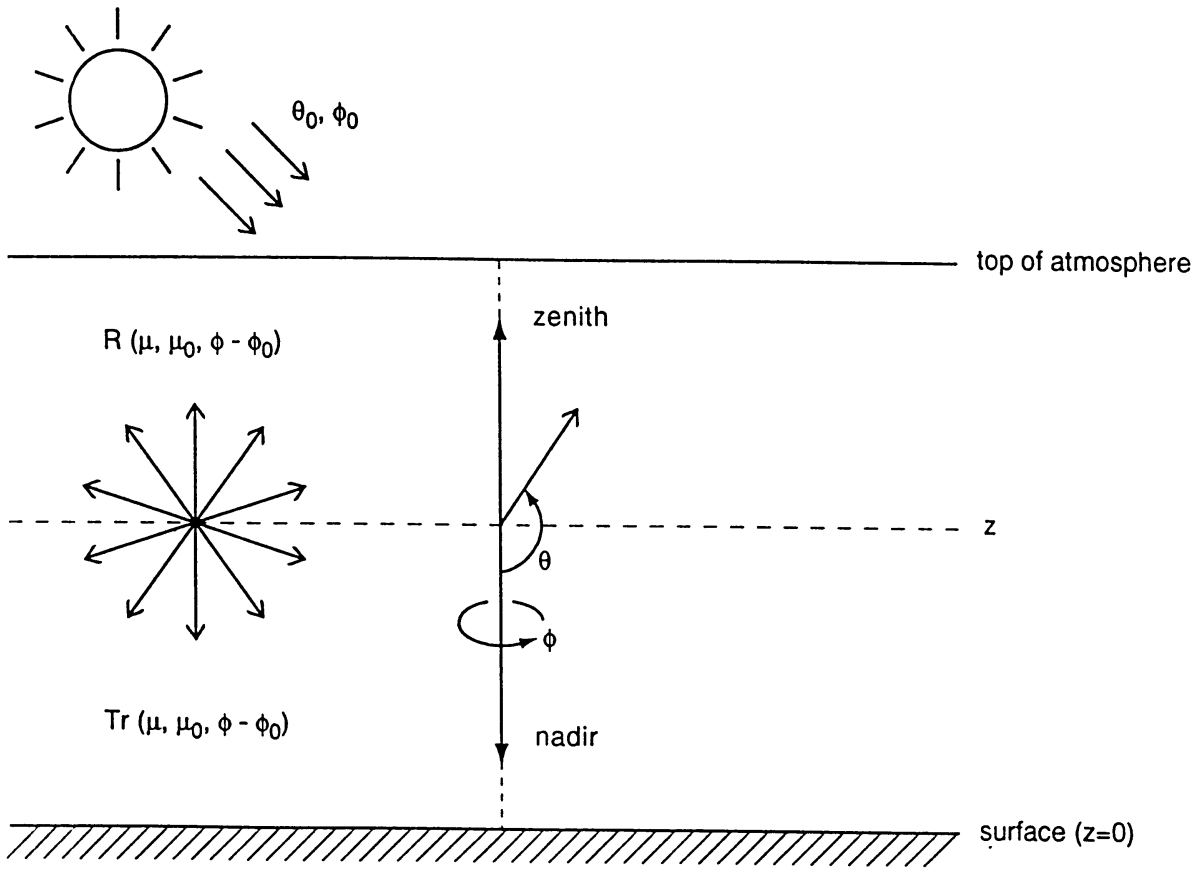

Figure 2. Definition of radiation directions. Radiation propagating in the atmosphere has a nadir angle θ and an azimuthal angle ϕ, counted clockwise when looking upwards. Downward radiation has $0 \leq \theta \leq \pi/2$, and upward radiation has $\pi/2 \leq \theta \leq \pi$. Incident sunlight is described by θ_0 and ϕ_0. We often use $\mu = |\cos\theta|$ and $\mu_0 = |\cos\theta_0|$. The functions $R(\mu, \mu_0, \phi - \phi_0)$ and $Tr(\mu, \mu_0, \phi - \phi_0)$ represent, respectively, the bidirectional reflection and transmission properties of a cloud.

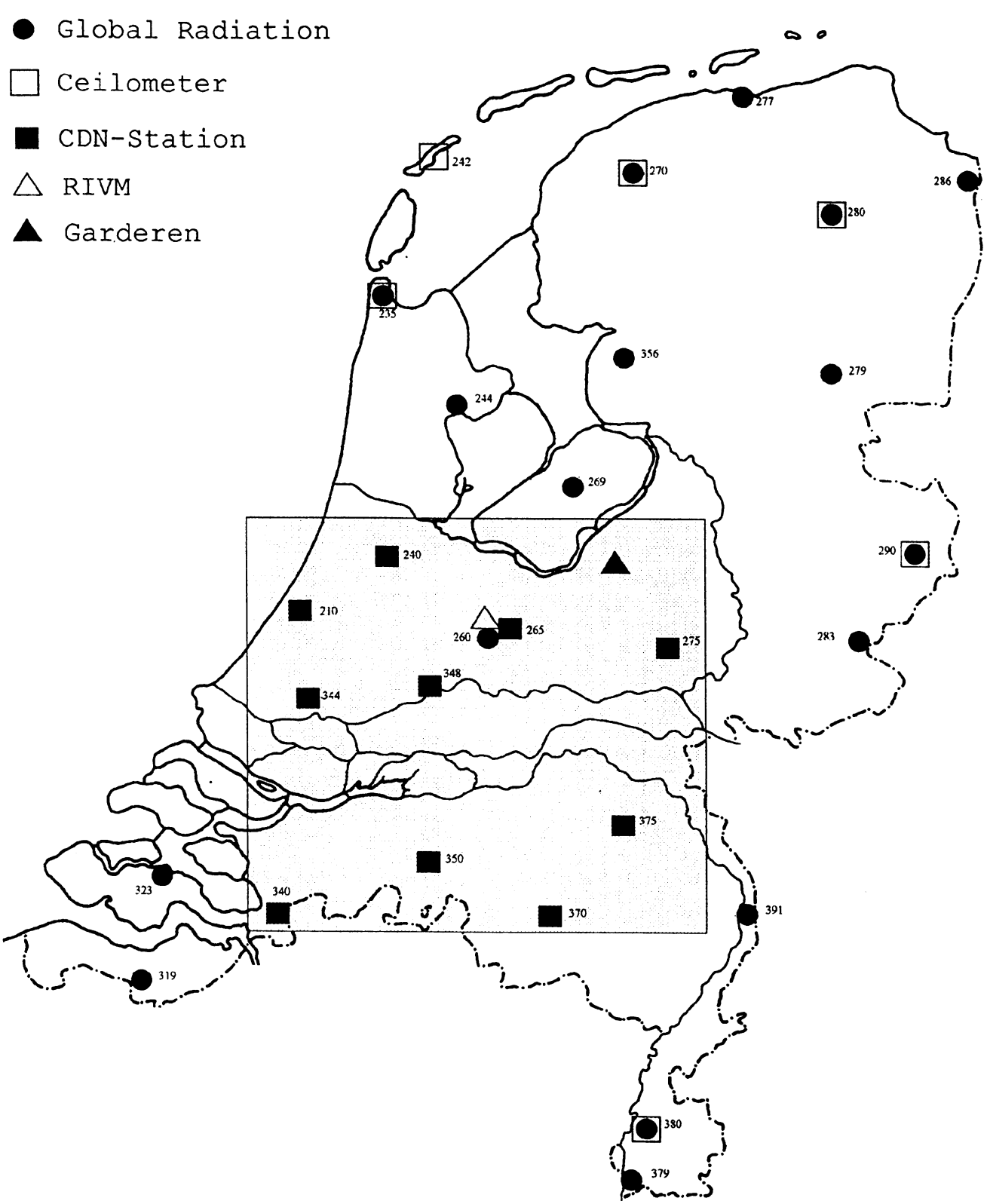

Figure 3. Ground network sites of cloud and radiation observations for TEBEX.

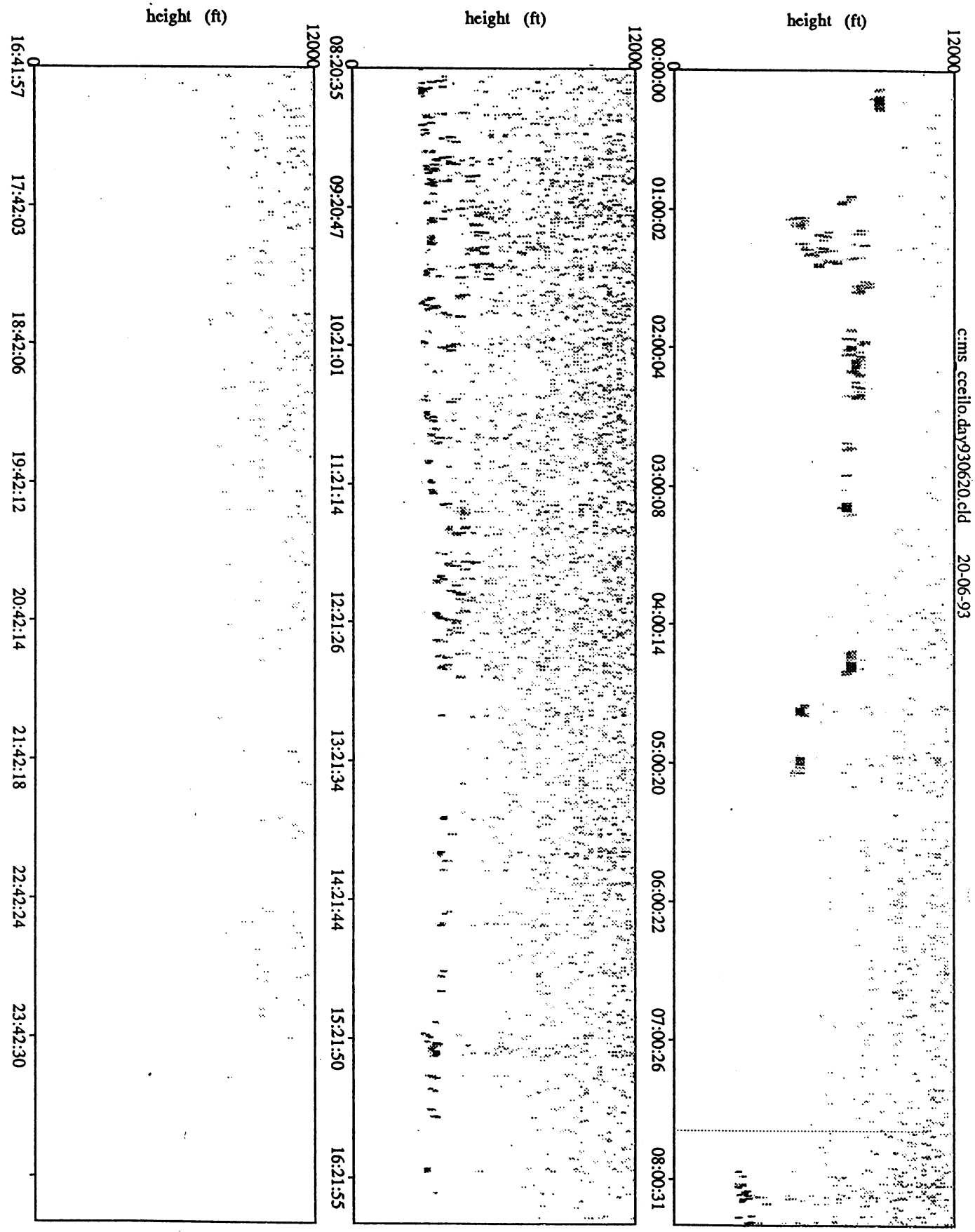

Figure 4. Example of lidar backscatter intensity measurements as a function of time (x-axis, in UT) and altitude (y-axis). Data obtained on 20 June 1993 with the ceilometer at Cabauw. From these data e.g. the cloud base height can be determined.

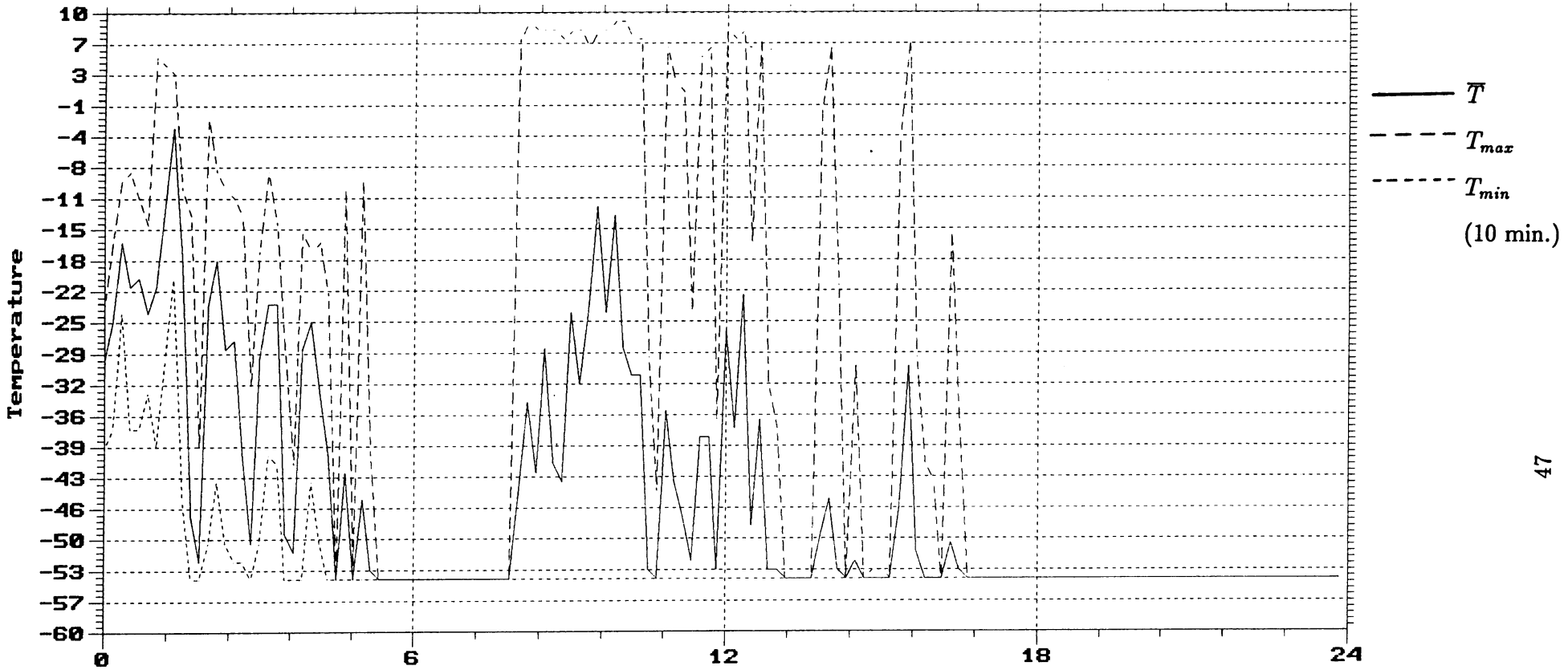

Figure 5. Example of sky brightness temperature measurements as a function of time (x-axis, in UT), obtained with the Heimann radiometer at Cabauw on 20 June 1993. Average ($\overline{T}$), minimum (T_{min}), and maximum (T_{max}) temperatures in 10-min. periods are given.

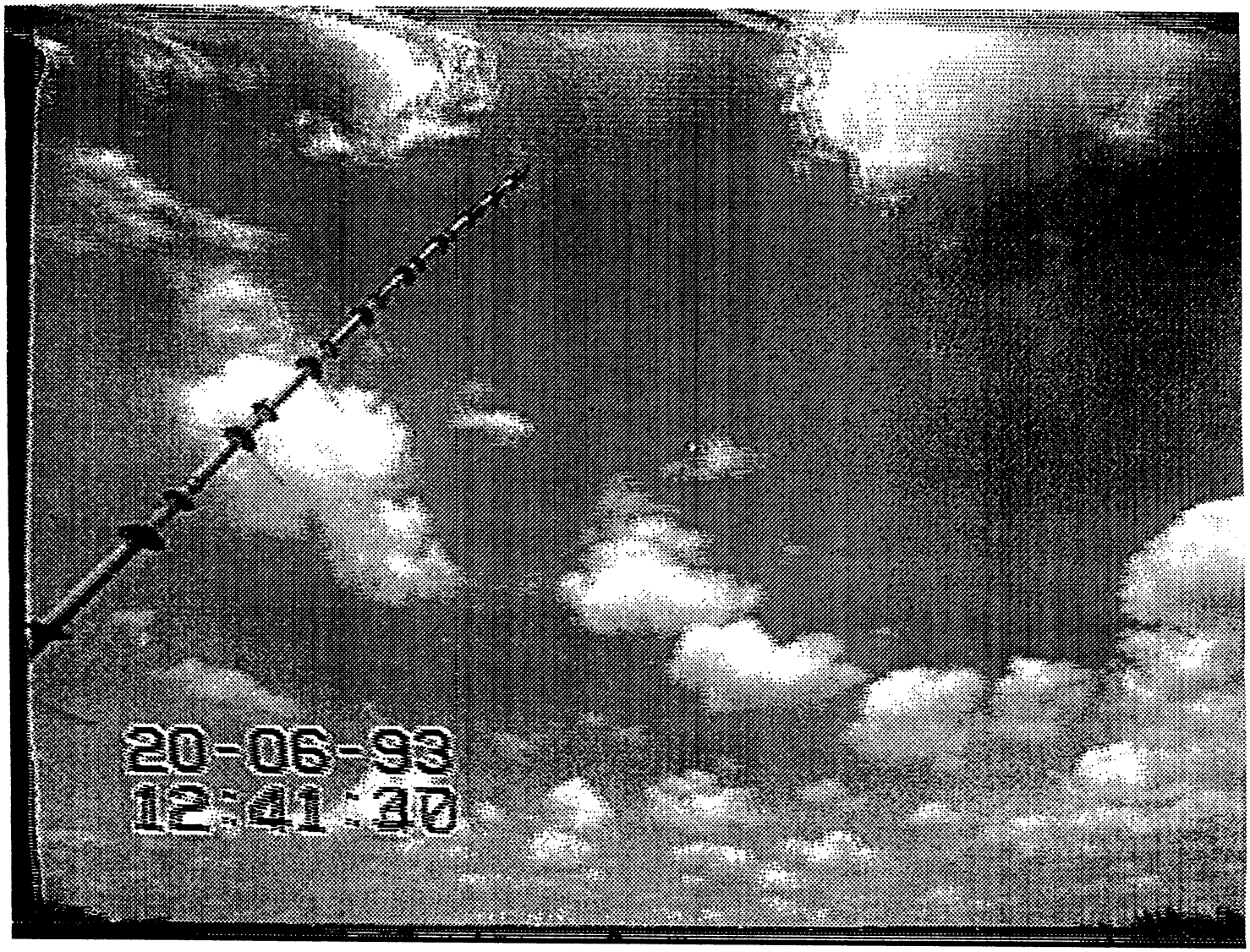

Figure 6. Example of a video-camera image, taken at Cabauw on 20 June 1993.

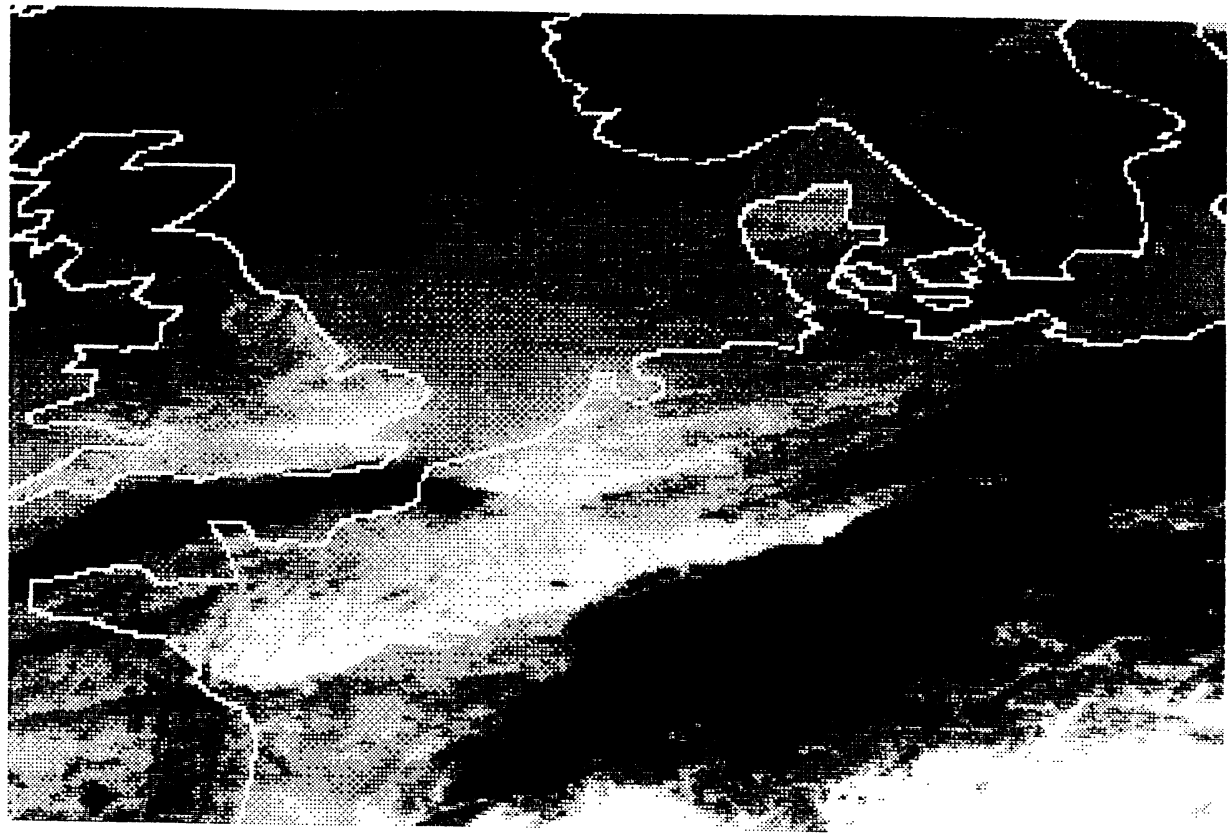

a

b

Figure 7. Meteosat image of North-West Europe on 20 June 1993 at 0830 UT. **(a)** IR channel: black corresponds to brightness temperature -15 °C or colder, white corresponds to +15 °C or warmer. **(b)** VIS channel: white corresponds to high, black to low reflectivity. The greyscale is arbitrary.

a

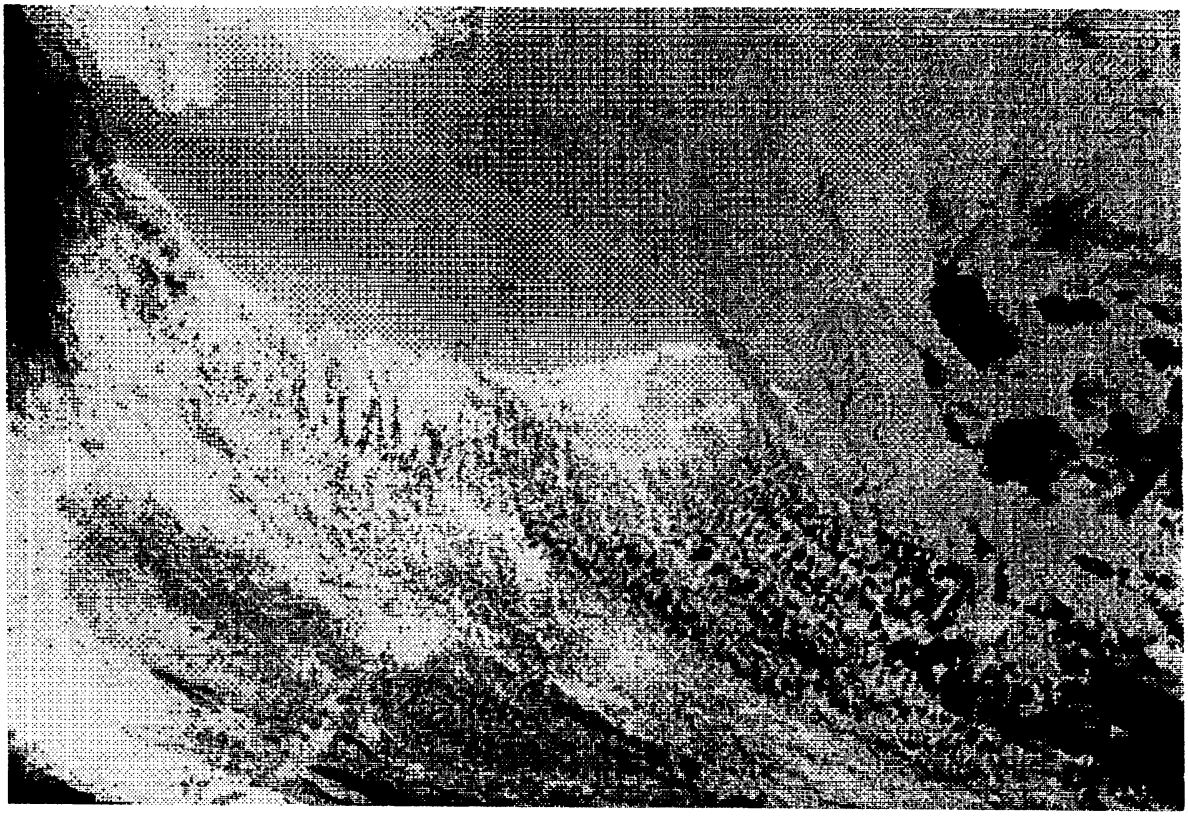

b

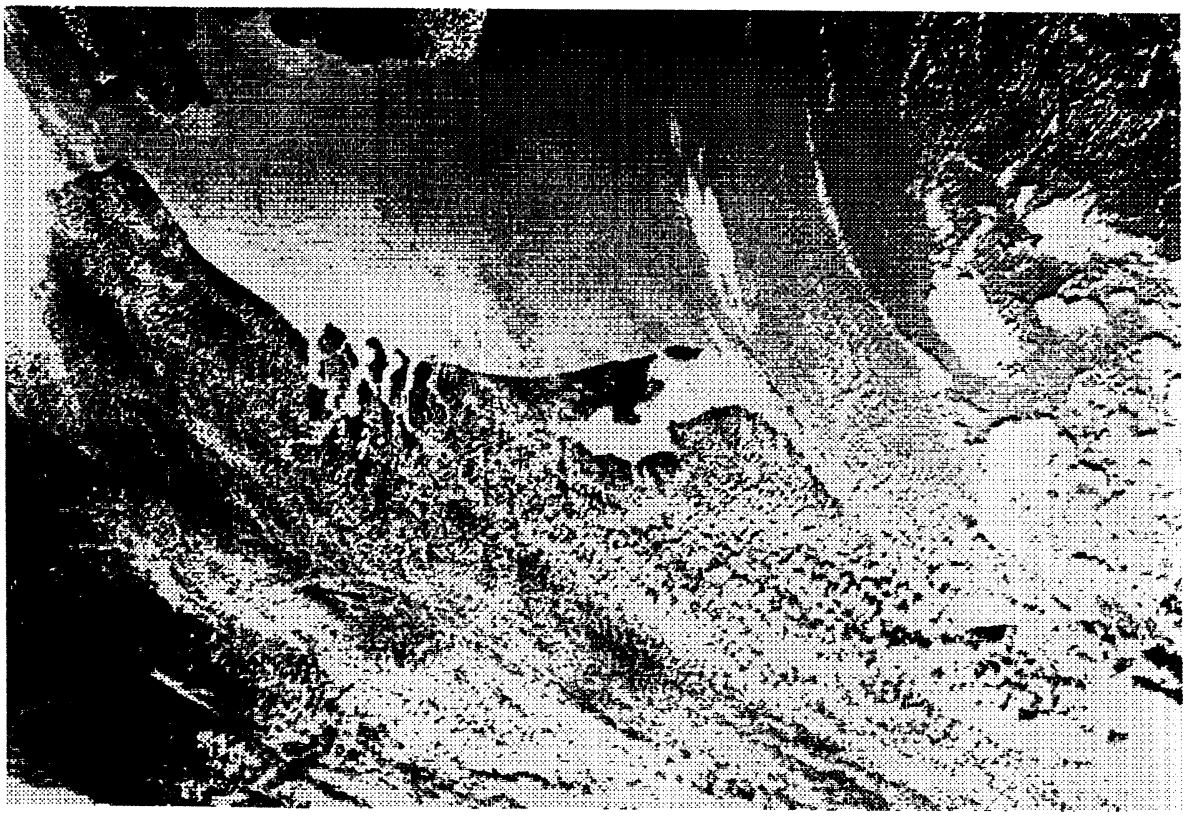

Figure 8. AVHRR image of the Netherlands on 20 June 1993 at 0827 UT. (a) Channel 4: black corresponds to brightness temperature -15 °C or colder, white corresponds to +15 °C or warmer. (b) Channel 1: white corresponds to high, black to low reflectivity. The greyscale is arbitrary.

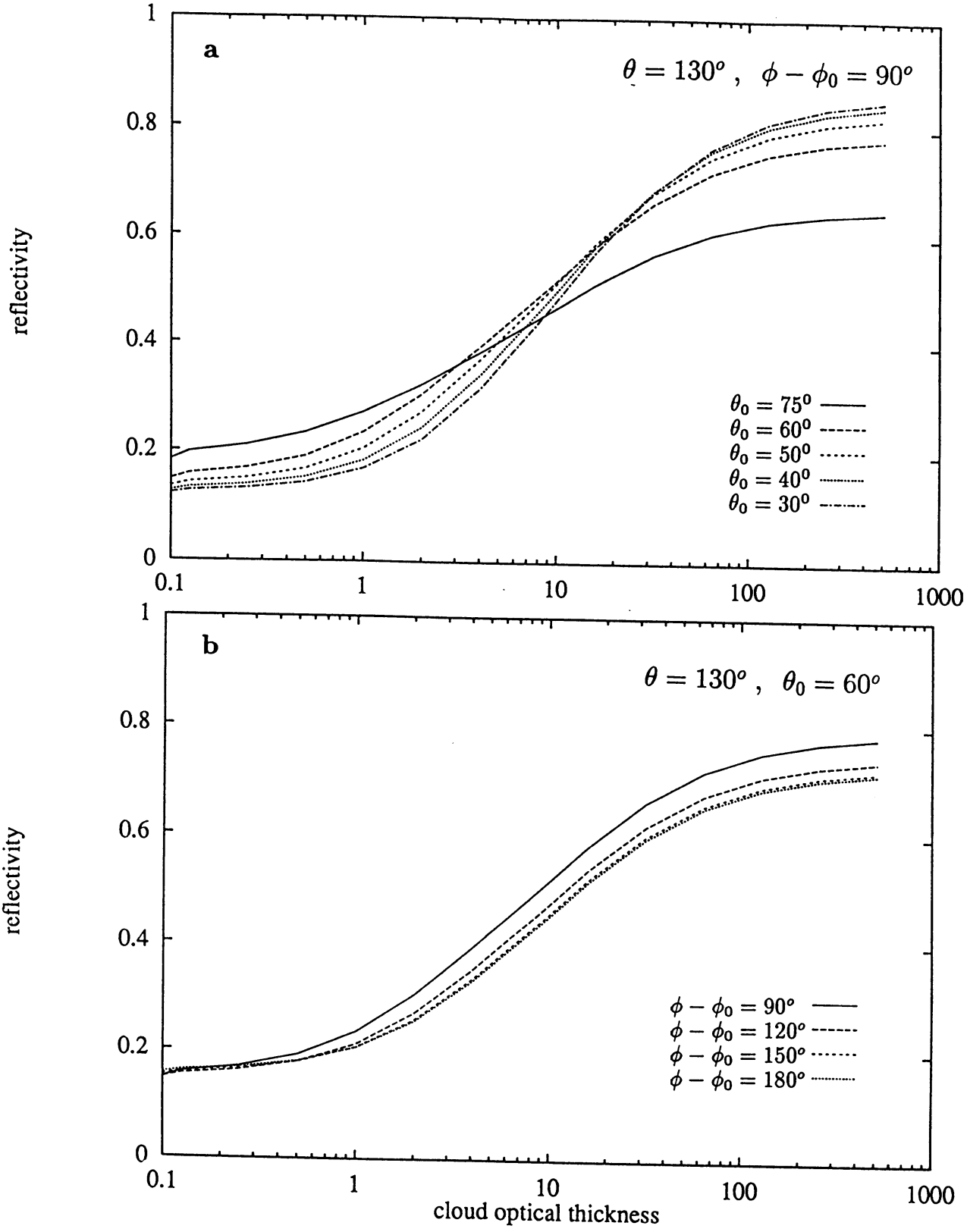

Figure 9. Bidirectional reflectivity R of the atmosphere at $\lambda = 0.6$ μm computed by the DAK model, as a function of cloud optical thickness, τ_0, for geometries relevant to the Meteosat view of the Netherlands.
(a) Geometry: $\theta = 130°$, $\phi - \phi_0 = 90°$, θ_0 varies.
(b) Geometry: $\theta = 130°$, $\theta_0 = 60°$, $\phi - \phi_0$ varies.
Atmospheric model: Mid-Latitude-Summer pressure and ozone profile; maritime aerosol in boundary layer, and background aerosol in free troposphere and stratosphere; cloud situated between 1 and 2 km, with single scattering albedo 0.999999 and asymmetry parameter 0.83; ground albedo 0.1.

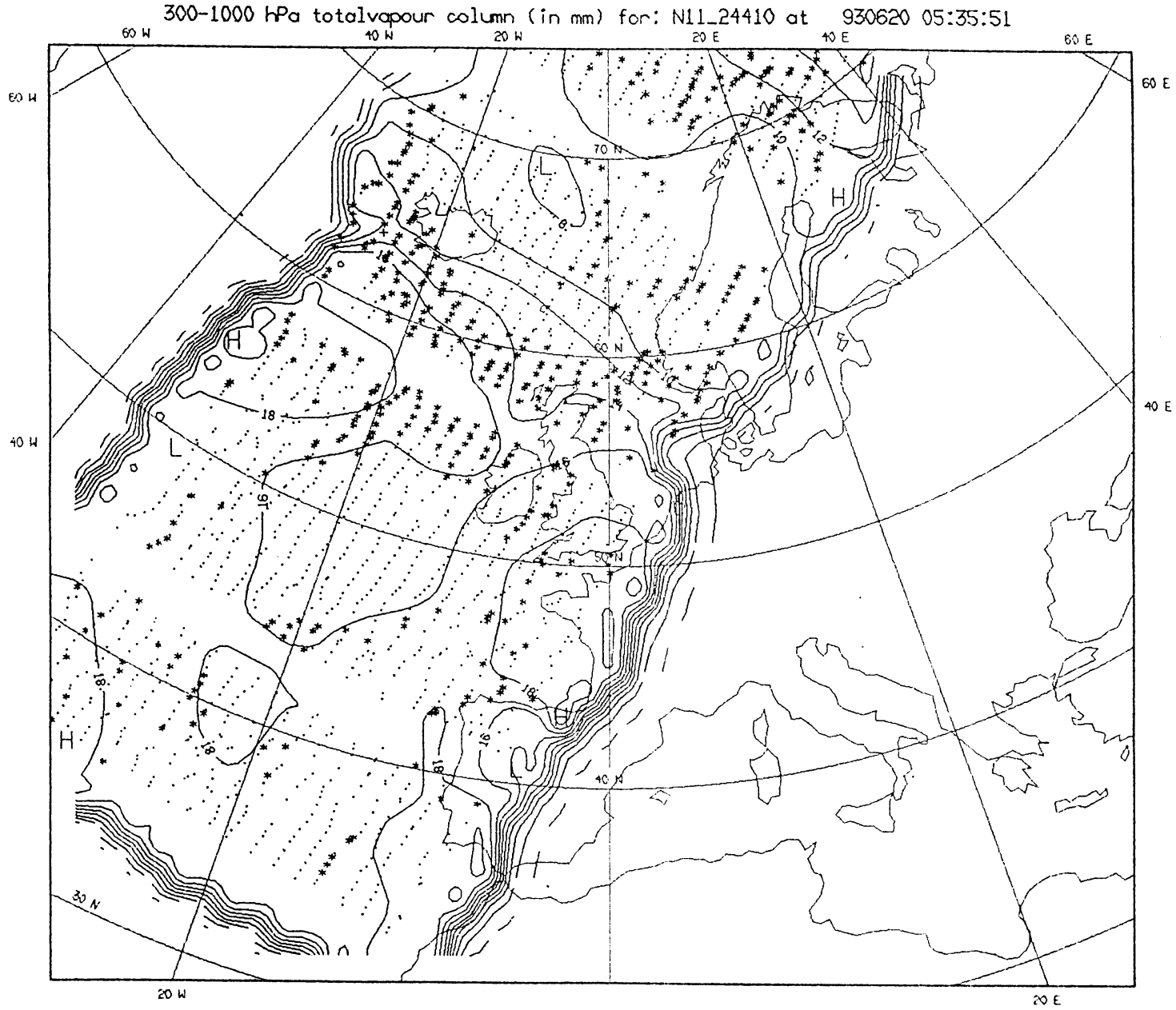

Figure 10. Water vapour column density (isolines, in mm) retrieved by the 3I method from TOVS radiances, for a NOAA-11 orbit on 20 June 1993. Dots denote good data, stars denote rejected data.